Geomorphology 214 (2014) 465–484

Contents lists available at ScienceDirect

Geomorphology

journal homepage: www.elsevier.com/locate/geomorph

Inner gorge–slot canyon system produced by repeated stream incision (eastern Alps): Significance for development of bedrock canyons

Diethard Sanders [a,*], Lukas Wischounig [a,1], Alfred Gruber [b], Marc Ostermann [a]

[a] Institute of Geology, University of Innsbruck, 6020 Innsbruck, Austria
[b] Geological Survey of Austria, Neulinggasse 38, 1030 Vienna, Austria

ARTICLE INFO

Article history:
Received 2 September 2013
Received in revised form 1 March 2014
Accepted 3 March 2014
Available online 12 March 2014

Keywords:
Alps
Quaternary
Canyon
Gorge
Slot canyon
Base level

ABSTRACT

Many inner bedrock gorges of the Alps show abrupt downstream changes in gorge width, as well as channel type and gradient, as a result of epigenetic incision of slot canyons. Many slot canyons also are associated with older gorge reaches filled with Quaternary deposits. The age of slot canyons and inner bedrock gorges, however, commonly is difficult to constrain. For the inner-bedrock gorge system of the Steinberger Ache catchment (eastern Alps), active slot canyons as well as older, abandoned gorge reaches filled with upper Würmian proglacial deposits record three phases of gorge development and slot–canyon incision. A $^{234}U/^{230}Th$ age of cement of 29.7 ± 1.8 ka in fluvial conglomerates onlapping the flank of an inner gorge fits with late Würmian valley-bottom aggradation shortly before pleniglacial conditions; in addition, the age indicates that at least the corresponding canyon reach must be older. During advance of ice streams in the buildup of the Last Glacial Maximum (LGM), the catchment was blocked, and a proglacial lake formed. Bedrock gorges submerged in that lake were filled with fluviolacustrine deposits. During the LGM, the entire catchment was overridden by ice.
During post-glacial reincision, streams largely found again their preexisting inner bedrock canyons. In some areas, however, the former stream course was 'missed', and a slot canyon formed. The distribution of Pleistocene deposits, the patterns of canyon incision, and the mentioned U/Th cementation age, however, together record a further discrete phase of base-level rise and stream incision well before the LGM. The present course of Steinberger Ache and its tributaries is a patchwork of (1) slot canyons incised during post-glacial incision; (2) vestiges of slot canyons cut upon an earlier (middle to late Würmian?) cycle of base-level rise and fall; (3) reactivated reaches up to ~200 m in width of inner bedrock gorge that are watershed at present, and more than at least ~30 ka in age; and (4) abandoned, sediment-filled reaches of bedrock canyons that also must be older than 30 ka and that are exposed alongside the active streams. 'Multi-cyclic' bedrock canyon systems composed of reaches of markedly different ages may be common in mountain ranges subject to glaciations and/or mass wasting.

1. Introduction

The incision of bedrock channels is one of the key processes in conceptual and numerical understanding of land surface development (Bishop, 2007). In the Alps, valleys with inner bedrock gorges ('gorge-within-valley') are common (Montgomery and Korup, 2011). Because they are loci of erosion, however, the potential age and incision history of inner bedrock gorges most commonly are difficult to deduce. Montgomery and Korup (2011) discussed two alternative explanations for development of the inner bedrock gorges of the Alps: (i) canyons formed completely anew after retreat of glaciers subsequent to full glaciation, or (ii) gorge excavation over successive glacial–interglacial cycles. Using LiDAR-based topography, they showed that if gorges had formed only after the Last Glacial Maximum (LGM), fluvial incision rates of ~8.5–18 mm/a – sustained over some 15–10 ka – were required to achieve present canyon depths. Montgomery and Korup (2011) argued that canyon cutting only after the LGM would require depths of glacial erosion that are inconsistent with thermochronometric data on exhumation, Quaternary denudation rates of the Alps, and the relative time available for glacial versus fluvial erosion over glacial–interglacial cycles. Within a number of gorges, deposits of the LGM or predating the LGM indicate that the canyon hosting the sediments must be older (Tricart, 1960; de Graaff, 1996; Ostermann et al., 2006; Montgomery and Korup, 2011). Therefore, Montgomery and Korup (2011) suggested that inner gorges in the Alps were typically excavated over several glacial–interglacial cycles. Furthermore, inner gorges entirely floored by, or containing lower reaches with, bedload channels from post-glacial sediment aggradation suggest that the incision, or continued incision, of these gorges proceeded underneath decaying ice streams (Dürst Stucki et al., 2012).

* Corresponding author. Tel.: +43 512 507 5584; fax: +43 512 507 2914.
E-mail address: Diethard.G.Sanders@uibk.ac.at (D. Sanders).
[1] Present address: Winklehner Geo Consultants, Moosgasse 38, 6065 Thaur, Austria.

http://dx.doi.org/10.1016/j.geomorph.2014.03.007
0169-555X/

Another aspect of repeated glaciations in mountain ranges is that they are associated with rapid and marked changes of local base levels (e.g., de Graaff, 1996; Reitner, 2007; Sanders, 2012). Because physical erosion is most effective shortly before and after cold climatic phases (e.g., Van Husen, 1983; Sanders and Ostermann, 2011; Tunnicliffe and Church, 2011), local base-level rises typically led to rapid sediment accumulation. As a result, valleys became clogged with sedimentary successions hundreds of meters in thickness. During and after deglacial ice decay, trunk valleys that were passed by ice streams and that were reamed out to some depth by subglacial erosion aggraded up to their present level (e.g., Bader, 1979; Van Husen, 1979; Preusser et al., 2010). In comparatively small, steep-gradient catchments, deglacial ice collapse initially led to a pulse of 'paraglacial' sedimentation (see, e.g., Church and Ryder, 1972; Orwin and Smart, 2004, for term) by redeposition of glacial drift and by production of copious amounts of hillslope clastic material. Subsequently, when the ratio of sediment delivery to watershed became smaller, the reincision of streams started (Sanders, 2012). During reincision, however, the previous stream network may not be found again along its entire extent, resulting in incision of epigenetic bedrock–canyon reaches, or slot canyons (Fig. 1). The term 'epigenetic' indicates that these canyon reaches are younger than the preexisting gorge (e.g., Penck and Brückner, 1901/1909; Ouimet et al., 2008). Slot canyons form by incision of stream channels that were laterally displaced, or that became abandoned or otherwise inactive, into bedrock spurs or flanks of the former valley rather than excavating the unconsolidated valley fill (Ouimet et al., 2008). Besides base-level changes associated with glacial–interglacial cycles, other common causes for slot canyon formation include landslides, alluvial fans, subglacial drainage, and anthropogenic changes such as mine tailings (e.g., Penck and Brückner, 1901/1909; Knauer, 1952; James, 2004; Hewitt, 2006; Korup et al., 2006; Pratt-Sitaula et al., 2007; Hewitt et al., 2008; Ouimet et al., 2008). Key differences between slot canyons and their hosting inner bedrock gorges are (i) the much shorter length of slot canyons relative to that of the entire gorge, and (ii) the fact that slot canyons are limited by a local base level set by the older gorge reach directly downstream. This base level may result from a previous longer term interplay of processes proceeding at rates that, in themselves, would not suffice to explain the depth of slot canyon cutting (cf. Montgomery and Korup, 2011). Documented rates of bedrock incision in slot canyon formation, in turn, can far outpace rates of overall landscape formation (e.g., James, 2004; Ouimet et al., 2008; Lamb and Fonstad, 2010).

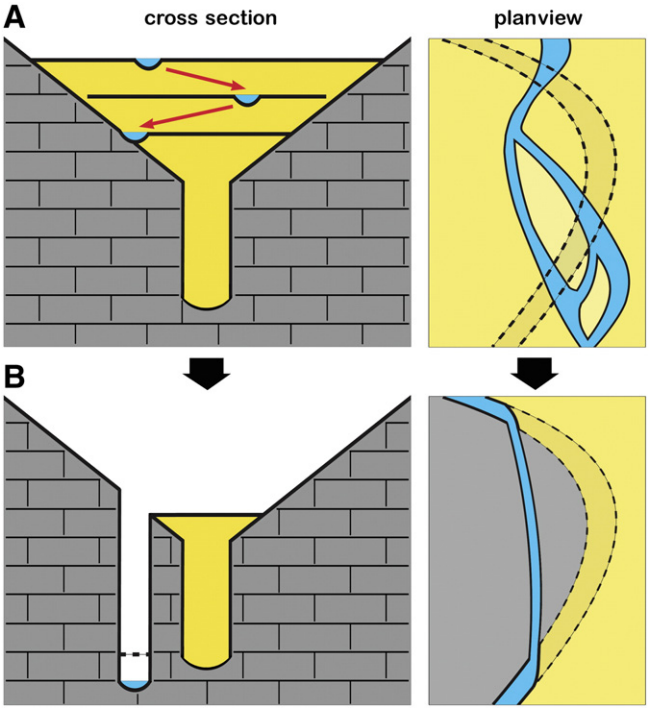

Fig. 1. Scheme of slot canyon development related to marked base-level rise by sedimentation (e.g., in a proglacial setting, as described herein). Sediment aggradation fills the valley, and clears the 'memory' of the stream for its former course. (A) In an early stage of reincision, the stream is free to shift laterally while downcutting until the older bedrock surface is encountered. (B) Upon continued reincision, some older bedrock reaches are hit again while others are missed, and a slot canyon is cut. The slot canyon may be incised to a similar depth (dashed line) or deeper than the preexisting gorge.

In the present paper, based on a detailed study of a catchment in the northern calcareous Alps (NCA), we describe bedrock dissection by repeated canyon incision (Fig. 2). At least the post-LGM phase of slot–canyon cutting was mediated by proglacial (pro-LGM) sediment aggradation that leveled out the relief of the inner bedrock gorge so as to erase the 'memory' of the post-glacial, downcutting stream network. For a still older phase of canyon cutting, no record of potential causes is preserved. The switches between sedimentation and incision produced a truncation surface of highly differentiated relief on top of the bedrock. In the NCA, epigenetic gorges are widespread, but the density of slot canyons observed in the area described herein seems to be rare. Our observations support the conclusion of Montgomery and Korup (2011) that many of the inner bedrock gorges of the Alps formed over several cycles of major base-level change.

2. Methodology

The study area was part of a larger scaled mapping campaign on a scale of 1:25,000 for the Geological Map of Austria (Gruber, 2011). The study area itself was previously field-mapped with respect to substrate geology, Quaternary sedimentary facies, and morphology on a scale of 1:5000 (Wischounig, 2006). A longitudinal stream profile was constructed via a three-dimensional polyline based on the 1-m contoured LiDAR-based digital terrain model of the federal government of Tyrol. A 3D polyline connects points in space, whereby each point is defined by its coordinates *x*, *y* and *z*. To arrive at a longitudinal stream profile with correct length, each point of the polyline was rotated into the two-dimensional section plane using a SCILAB script (www.scilab.org). After import of the 2D profile into a CAD model, the profile was redrawn with 10 times vertical exaggeration. A local anthropogenic change in stream course (see below) was backtracked by means of historical maps (link 'Historische Kartenwerke Tirol' at http://tiris.tirol.gv.at/) and by the records of the Austrian Service of Torrent and Avalanche Control.

Quaternary sediments were documented in key outcrops and by 16 logged sections. Lithified Quaternary deposits were inspected in cut slabs and thin sections. Samples of fine-grained lacustrine sediments were investigated for mineralogical composition by X-ray powder diffractometry (Wischounig, 2006; Gruber et al., 2011a). X-ray diffractometric analyses were performed on a Bruker-AXS D8 diffractometer (Bragg-Brentano geometry), CuKa radiation at 40 kV and 40 mA acceleration voltage, with parallel-beam optics and an energy-dispersive detector. The data was collected between 2 and 70° 2θ, with a step size of 0.02° 2θ and a detecting time of 4 s per step. Crystalline phase identification was achieved with the program Eva.Ink and the PDF4 data base 8.0.113 of ICDD. The X-ray spectra were analyzed with the programs DIFFRAC PLUS (phase identification) and TOPAS (quantitative assessment).

An isopachous fringe of calcite cement within a fluvial conglomerate was age-dated by the $^{234}U/^{230}Th$ disequilibrium method (Ostermann, 2006). The calcite cement was sampled with a microdrill and cleaned physically as far as possible. Samples were spiked with a mixed $^{236}U + {}^{229}Th$ spike and dissolved in HNO_3, after which remaining organics were attacked with $H_2O_2 + HNO_3$. Separation of U and Th was done with 0.5 ml Eichrom™ U-Teva® resin. Analyses of U and Th were performed separately on an Nu-instruments™ MC-ICP mass

spectrometer. ^{236}U and ^{234}U were measured in separate electron multipliers (static mode). Thorium measurements were done in dynamic mode, by alternate measurement of ^{230}Th and ^{229}Th in the same multiplier. For thorium measurements, to control electron multiplier gain the MOSS (Be Inhouse) standard was used. For gain calibration of U, the NIST U 050 standard was taken. To correct for detrital contamination, the regression line ('isochron') method with several subsamples was chosen (e.g., Ludwig and Titterington, 1994; Lin et al., 1996; Frank

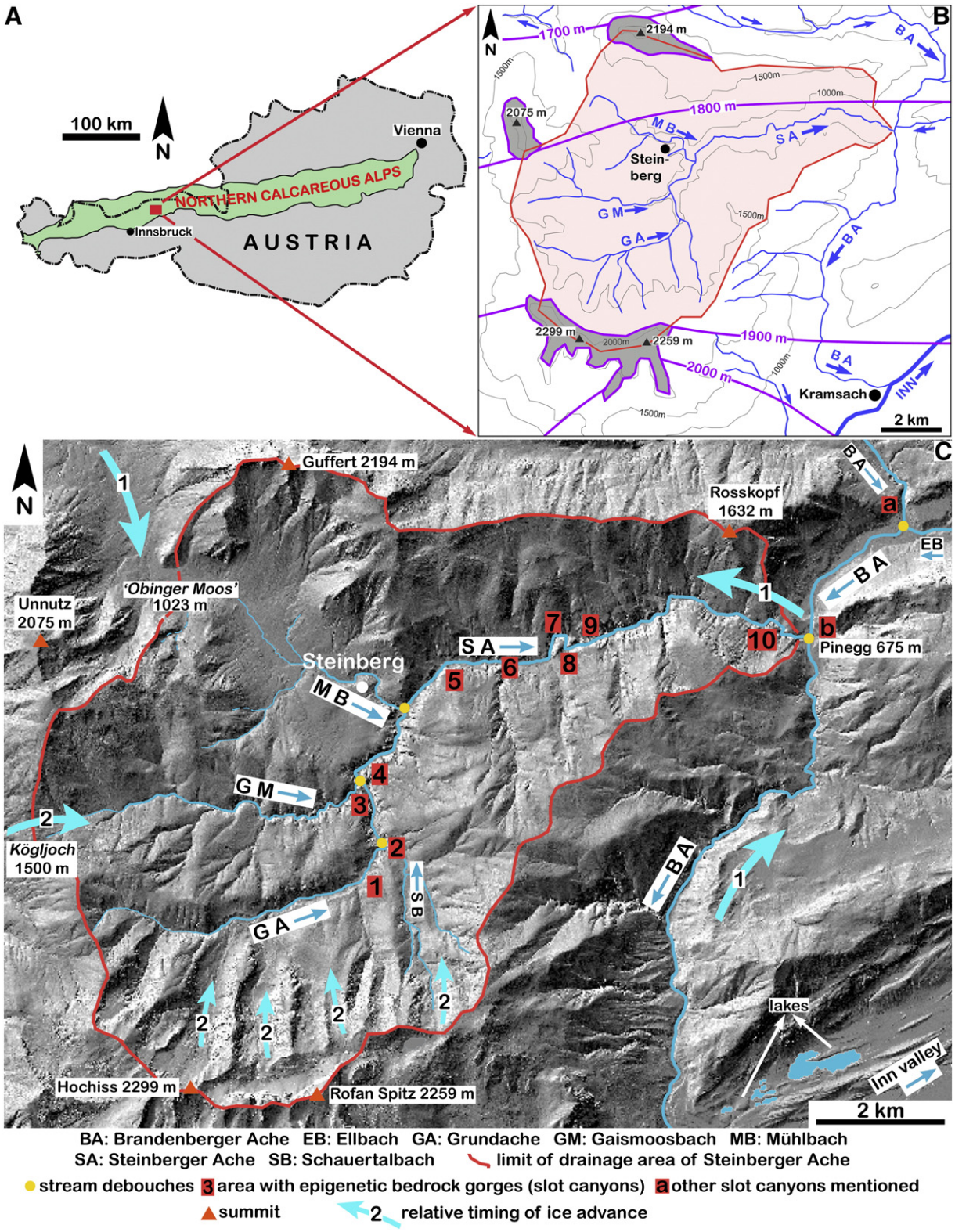

Fig. 2. (A) Geographic location of the study area (red rectangle) in the northern calcareous Alps (light green). (B) Map of Steinberger Ache catchment, with reconstructed ice surface of the Last Glacial Maximum (after Van Husen, 1987). During the Last Glacial Maximum, except for three nunataks, the catchment was buried by an overall northward-flowing ice stream. (C) Laserscan image showing catchment of Steinberger Ache (SA; red outline), and its connection to the trunk valley of the Inn River via Brandenberger Ache (BA).

et al., 2000). The activity ratios of U and Th isotopes were plotted in diagrams ('Osmond plots', 'Rosholt plots') to (i) calculate activity ratios corrected for detrital contamination and (ii) to identify subsamples that potentially had reopened after closure (e.g., Osmond et al., 1970; Rosholt, 1976; Frank et al., 2000; Geyh, 2001, 2005, 2008) (see Ostermann et al., 2006, for detailed description of method). For age calculation, the corrected activity ratios were fed into a Th–U disequilibrium age calculation program (Visual Basic, written by Jan Kramers (formerly at University of Berne, Switzerland), according to the equation of Kaufman and Broecker, 1965).

Our identification of slot canyons was based on the following criteria. (i) Slot canyons are much narrower than the corresponding up- and downstream reaches of the older, inner bedrock gorge. (ii) The rock cliffs along the flanks of the relatively wide, old inner bedrock gorges are weathered and lichenized and are devoid of surface features produced by fluvial erosion. Conversely, the flanks of slot canyons show an undulating, cuspate surface produced by incision of bedrock channels. (iii) Except for local accumulations of gravels to small boulders in plunge pools and potholes, slot canyons are floored by bedrock channels and may contain waterfalls. (iv) All of the slot canyons described herein are located adjacent to reaches of older, inner bedrock gorges filled by sediments. Herein, the term knickpoint is used to designate an abrupt change in stream gradient that is associated with a discrete channel reach with high gradient rapids, bedrock-incised step-pool and/or cascade channels, or waterfalls (cf. Gardner, 1983; Seidl et al., 1994; Whipple and Tucker, 1999; Bishop et al., 2005; Crosby and Whipple, 2006; Frankel et al., 2007). For practical reasons, we herein use the term bedrock channel for: bedrock channels sensu stricto (channels devoid of any sediment patches also at low stage) and bedrock channels with patches – typically in potholes or plunge pools – of gravels to cobbles at low stage (see Montgomery and Buffington, 1997; Whipple, 2004, p. 153); the latter would correspond to a mixed bedrock–alluvial channel (cf. Whipple and Tucker, 2002; Whipple, 2004). The descriptive terminology of bedrock channels is according to Wohl and Merritt (2001).

3. Setting

3.1. Northern calcareous Alps

The northern calcareous Alps (NCA; Fig. 2) are part of the eastern Alps and consist of a stack of cover-thrust nappes mainly of Triassic shallow-water platform carbonates. The nappe stack was formed during latest Jurassic to Paleogene orogenic convergence (e.g., Schmid et al., 2004). During the late Paleogene to early Neogene, large parts of the eastern Alps became subject to uplift and subaerial erosion. Until ~20 Ma most of the mountain range may have drained northward (Frisch et al., 1998; Kuhlemann et al., 2006). In the eastern part of the eastern Alps, small erosional vestiges of fluvial deposits ('Augensteine') above a truncation surface cut into deformed older rocks are tentatively interpreted as indicators of southerly shedding braid plains or piedmont bajadas (cf. Frisch et al., 2001). In the eastern Alps, the development of a comparatively straightforward drainage pattern was precluded by (i) superposed fold and fault structures resulting from shortening along different strain directions (cf., e.g., Decker et al., 1993; Eisbacher and Brandner, 1996), and (ii) Neogene disintegration and E–W lateral escape of the orogen along large strike-slip faults that trend parallel to oblique to the main crestline (e.g., Ratschbacher et al., 1991; Linzer et al., 1995; Wang and Neubauer, 1998; Fügenschuh et al., 2000; Rosenberg et al., 2004). Strike-slip faulting mediated the incision of major longitudinal valleys, such as the Inn valley (Fig. 2) (Ratschbacher et al., 1991; Ortner and Stingl, 2001; Robl et al., 2008a, b). Kuhlemann (2007) suggested that the paleocourses of the major longitudinal streams that presently drain the eastern Alps, including the Inn River, started to form at ~13 Ma. Whereas Neogene clastic foreland successions record some departures of the present from the former stream courses, they confirm that drainage along the major fault-controlled valleys prevailed ever since (Kuhlemann et al., 2002; Dunkl et al., 2006). The fault-controlled streams persisted as the major drainage conduits over Pliocene to Quaternary times, but their history of incision and switches of course before exiting the Alps still are poorly documented (Robl et al., 2008a,b). In the Alps, major glaciation and glacial shaping of the landscape by waxing and waning of ice streams probably started at 0.87 Ma (Muttoni et al., 2003). Over the entire Alps, the total isostatic rock uplift in response to Quaternary glacial erosion is modeled up to ~250 m along the axial zone, fading out toward the margins (Sternai et al., 2012). Quantitative reconstructions of pre-0.87 Ma stream-channel steepness and glacial erosion suggest (i) an increase of topographic relief and concavity of valley profiles, and (ii) a widespread increase in the elevation of peaks and ranges; only in the marginal parts of the Alps, including large parts of the NCA, peaks and ranges may have remained of roughly similar elevation as today (Sternai et al., 2012).

During the Quaternary, the eastern Alps were subject to at least four major glaciations (Van Husen and Reitner, 2011). Upon advance of ice streams supplied by large high positioned catchments, many tributary valleys were blocked (Van Husen, 2000). As a result, thick proglacial fluviolacustrine successions accumulated in blocked valleys before these were buried under ice (e.g., Van Husen, 1977, 2000; Ostermann et al., 2006; Reitner, 2007). In the eastern Alps, the LGM lasted from ~26.5 to 21 ka (see Preusser, 2004; Monegato et al., 2007; Starnberger et al., 2011). The LGM was followed by rapid meltdown of stagnant ice streams. This 'early late-Glacial ice decay' (ELGID) lasted from about 21 to ~19 ka BP, and reduced ice streams to about 50% of their LGM volume (Van Husen, 2004; Reitner, 2007). The ELGID was followed by the late-Glacial from ~19 ka to the onset of the Holocene at 11.7 ka BP (cf. Severinghaus et al., 1998). In the internal part of the eastern Alps (= central Alps), the late-Glacial was characterized by stadial phases with progressively smaller outreach of valley glaciers (Van Husen, 2004; Ivy-Ochs et al., 2006, 2009). In the NCA, however, the record and the age assignment of stadial advances still are highly uncertain (Hirtlreiter, 1992; Hanns Kerschner, Institute of Geography, University of Innsbruck, personal communication, 2012).

3.2. Catchment of Steinberger Ache

Steinberger Ache is a tributary to Brandenberger Ache that, in turn, debouches in the Inn River (Fig. 2). The catchment of Steinberger Ache is nearly entirely located on Triassic platform rocks (Fig. 2). Only along the southernmost fringe of the study area, in the north-facing cliffs of mount Hochiss and Rofan Spitz, Jurassic deep-water limestones and cherts are exposed. The Jurassic succession hosts diverse lithologies identifiable in the field as clasts down to fine gravel size (Table 1 in Supplementary material). The present course of Steinberger Ache and its main tributaries are characterized by inner bedrock gorges up to 100–150 m wide, changing downstream with slot canyons about 1 m to a few meters in width along their base. Upslope of the inner gorges and canyons, the mountain flanks are of similar steepness, and of similar variability in steepness, as in other areas of the NCA.

In the western NCA, the late Middle Würmian (MIS 3; 61–29 ka; Martinson et al., 1987) was characterized by a cool climate and a tundra-like vegetation. During the later part of MIS 3, from at least ~36 to 27 ka, thick fluvial and fluviolacustrine successions accumulated along the Inn valley and along its tributaries (e.g., Fliri et al., 1970; Poscher, 1994; Reitner, 2007, 2011; Starnberger et al., 2011). The lower reach of the Inn valley probably was devoid of glacial ice until at least 27 ka BP (Reitner, 2011). Significant fluvial sediment aggradation between ~36 and 27 ka perhaps largely resulted from increased physical weathering and sparse vegetation rather than from valley blockade by advancing ice streams (Reitner, 2011; cf. Van Husen, 1983). As outlined below, U/Th dating of cement in fluvial deposits of the pre-LGM Grundache stream indicates that an inner bedrock gorge already

existed during the late MIS 3 phase and that this gorge underwent partial infilling from valley bottom aggradation that may be assigned to this phase (Figs. 2 and 3).

During buildup of the LGM, an advancing branch of the combined Inn–Ziller glacier blocked Steinberg valley from the east; at a similar time or perhaps shortly later, a branch of the Inn glacier advanced via Obinger Moos from the northwest (Fig. 2). Drainage thus was blocked, and a proglacial lake dubbed Lake Steinberg formed (Ampferer, 1905; von Wolf, 1922; Horvacki, 1982; Gruber et al., 2011b). Sediment aggradation in proglacial Lake Steinberg was punctuated at least once by marked lake-level lowering and associated fluvial incision (see Fig. 3, and farther below). In individual outcrops, the proglacial fluviolacustrine successions are up to ~100 m in thickness (Fig. 4). The level of Lake Steinberg attained an elevation of at least 1100 masl (highest preserved foreset beds; section C, Fig. 4), well above most of the present catchment area of Steinberger Ache. The pre-LGM drainage system thus was leveled out by fluviolacustrine sediment accumulation (Ampferer, 1905; Wischounig, 2006). In the study area, the reconstructed LGM ice surface ranged from 1900 masl in the south to 1750 masl in the north. As a result, except for the nunataks of Guffert, Unnutz, and the northern Rofan summits, the area was overridden by ice (Fig. 2B) (cf. Van Husen, 1987; Gruber et al., 2011a).

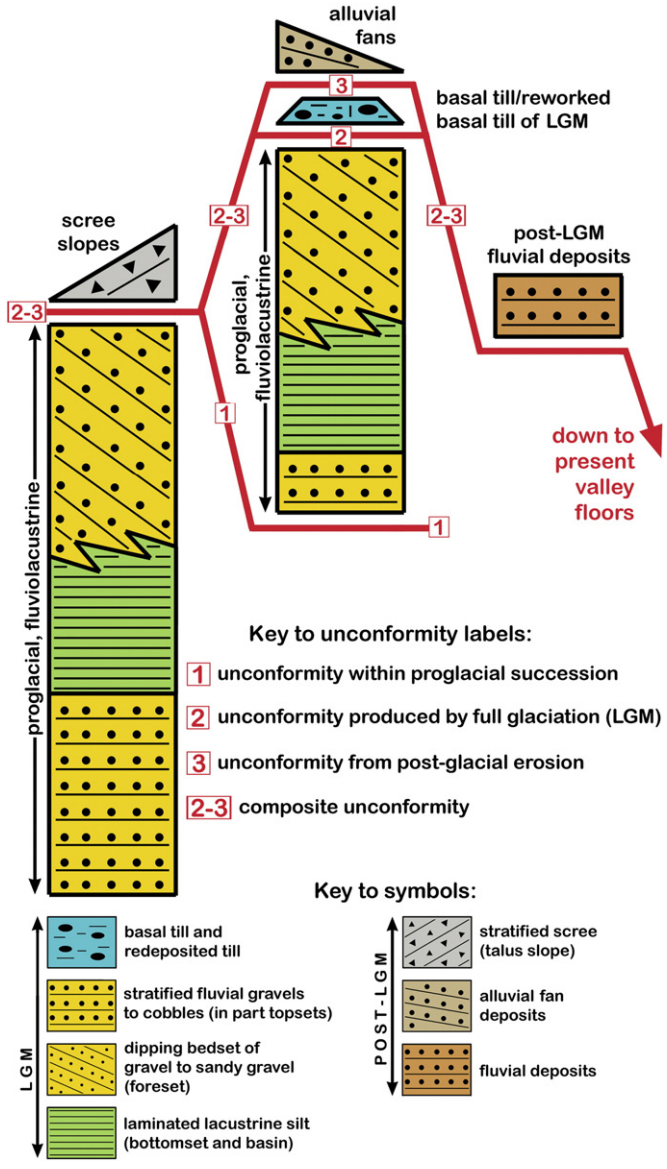

Fig. 3. Schematic summary of Quaternary sediment record. Valley-bottom sedimentation started during the latest Würmian, probably somewhere between ~36 and 27 ka BP (see text). These valley-bottom deposits are patchily cemented and are sharply overlain by a proglacial fluviolacustrine succession. The proglacial succession accumulated during advance of ice streams (cf. Fig. 2C) that blocked the inner bedrock canyons of the catchment. The proglacial succession contains at least one intraformational unconformity. During the LGM, the area was overridden by glacial ice (unconformity 2). During to shortly after ice collapse, strong erosion (unconformity 3) cannibalized most of the glacial till and incised into the pre-LGM succession. Locally, unconformity 3 became overlain by deposits of late-glacial to early Holocene age, such as scree slopes, alluvial fans and fluvial sediments. See Table 2 in Supplementary material for further characterization of proglacial to pleniglacial deposits.

Subsequent to the LGM, perhaps during the Gschnitz Stadial (~17–15 ka; Ivy-Ochs et al., 2008), glaciers of east- and north-facing cirques (north slope of Rofan massif, east slope of Unnutz) advanced down to near Obinger Moos (1000–1100 masl) and upper Grundache valley (c. 1000–1300 masl) (Van Husen, 2004; Wischounig, 2006; Gruber, 2008). The glacial advance led to another pulse of sediment input to the upstream reach of Grundache (upstream of slot canyon #2; see Fig. 2C). The question of post-LGM onset of stream reincision is discussed in more detail farther below. There is no evidence that local cirque glaciers nucleated and advanced during stadials subsequent to the Gschnitz Stadial. In the central Alps, glaciers of the Egesen stadial (probably equivalent with the Younger Dryas) terminated at about 1900–2000 masl, and glaciers of the Kromer stadial (perhaps equivalent with the 8.2 ka event) terminated at 2100 masl and higher (Kerschner et al., 2006; Ivy-Ochs et al., 2008). For the study area, it is thus highly improbable that glaciers, if present at all, came even near to valley floors after the Gschnitz stadial (Van Husen, 2004; Gruber et al., 2011b).

By analogy with the Inn valley adjacent to the south (Fig. 2), reforestation in the study area may have started at ~16–15 ka BP (cf. Patzelt, 1980; Van Husen, 2004). Upward climb of vegetation progressively slowed physical weathering and scree production and stabilized mountain flanks. Consequently, because of decreasing sediment input, the geomorphic regime changed to incision (cf. Sanders and Ostermann, 2011; Sanders, 2012). Today, in the catchment, active scree slopes all are located higher than an 'outlier' minimum of 1640 masl (toe of lowest active scree slope), well above the altitude range of 675 masl (Pinegg) to 1500 masl (area near Kögljoch) of interest herein (cf. Fig. 2C). During the late-Glacial changeover from sedimentation to incision, Steinberger Ache and its tributaries had largely hit again their pre-LGM inner bedrock gorges. Along these older reaches, the reincising streams cleared out the pre-LGM fluviolacustrine succession. Along some reaches, however, the reincising streams 'missed' their pre-glacial course. In consequence, a bedrock slot canyon was incised. The present course of Steinberger Ache and its tributaries thus is a 'chain' of bedrock canyons formed (i) before the LGM, changing downstream with (ii) slot canyons incised after the LGM (Sanders et al., 2006). In area 4 of slot canyon incision (Fig. 2C), the stream course was changed by human interference. This disturbance, described farther below, does not detract from the reconstructed natural development of repeated cutting, or deepening, of bedrock gorges. Herein, emphasis is placed on development of stream course in relation to cycles of base-level change. Quaternary sedimentary facies, described previously (Ampferer, 1905; Horvacki, 1982; Wischounig, 2006; Gruber et al., 2011a,b), in the following are treated only briefly as pertinent for the topic of this paper.

4. Quaternary sediment record

The Quaternary of the study area can be subdivided into three major parts (cf. Figs. 3 and 4): (i) a fluviolacustrine succession accumulated shortly before the LGM, and during the existence of Lake Steinberg; (ii) glacial till of the LGM, and (iii) deposits of the deglacial to post-glacial phase, mainly (i) kames terraces and paraglacially redeposited till, (ii) proximal fluvial deposits exposed along terraces flanking present streams, (iii) alluvial fans and scree slopes, and (iv) lateral and terminal moraines of local glaciers that probably nucleated and advanced during the Gschnitz stadial.

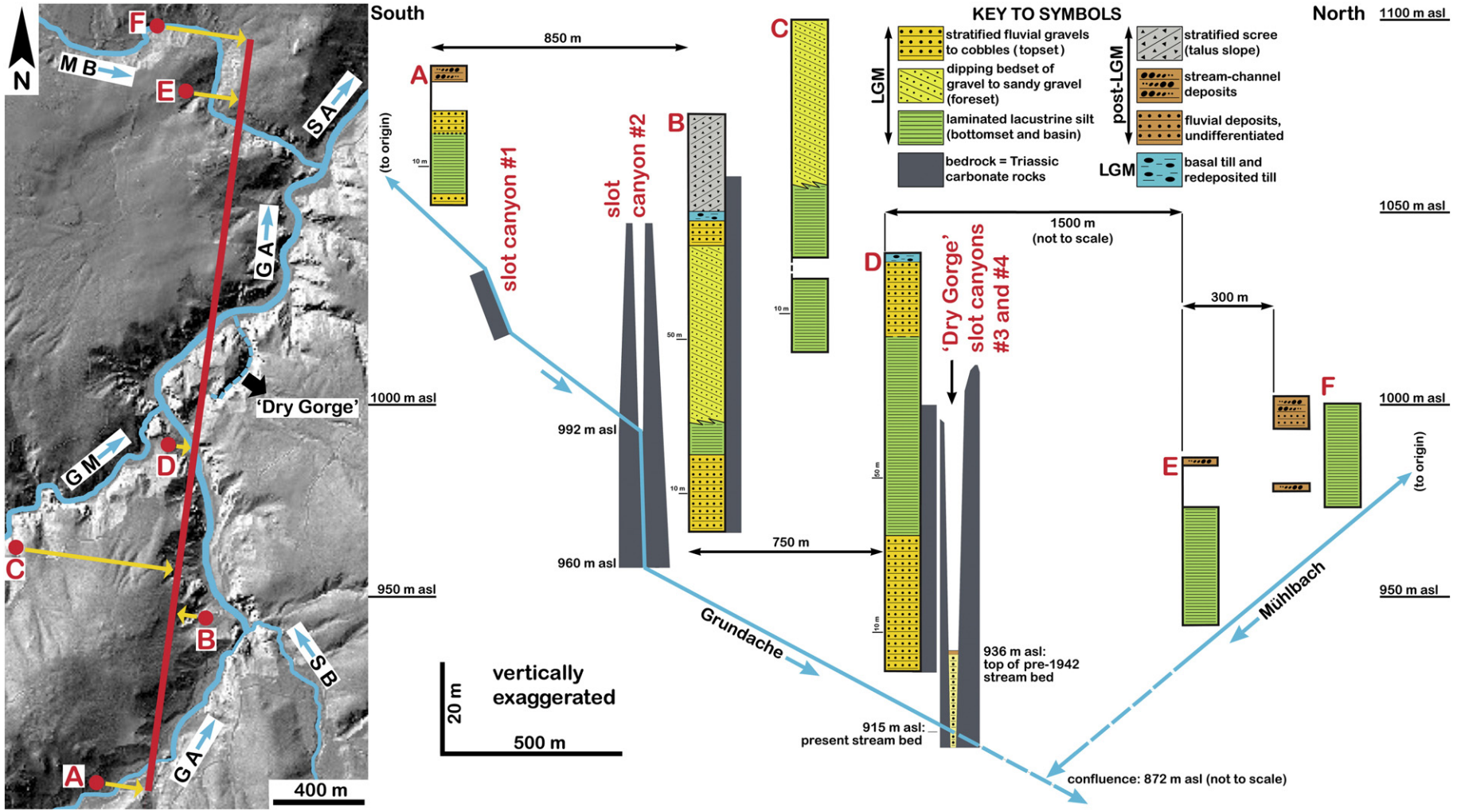

Fig. 4. Correlated sections from Grundache to Mühlbach (see Fig. 2C for area) showing Quaternary deposits, unconformities, pre-LGM bedrock-valley flanks onlapped by proglacial successions and the relative position of post-LGM slot canyons. The preserved top of the highest located foreset package is at 1100 masl (section C). Note strong vertical exaggeration. GA: Grundache; GM: Gaismoosbach; SA: Steinberger Ache; SB: Schauertalbach.

Within the inner bedrock gorges, the oldest preserved Quaternary sediments include subhorizontally stratified fluvial gravels to gravelly sands composed exclusively of lithoclasts derived from the NCA. These deposits were locally observed up from the present stream levels in the inner gorges of Grundache and Steinberger Ache (cf. Figs. 2C and 3). They are sharply overlain by the fluviolacustrine succession of Lake Steinberg that comprises the majority of the sediment infilling the pre-LGM inner bedrock gorges. The most widespread facies of Lake Steinberg comprise parallel-laminated silty muds and silts (subsumed as 'banded silts'). The banded silts consist of variable relative proportions of clastic carbonate minerals (calcite, dolomite) derived from the NCA rock substrate and, subordinately, of siliciclastic minerals; the latter were derived from the advancing ice streams and, perhaps, also from aeolian input (Horvacki, 1982; Wischounig, 2006; Gruber et al., 2011a). In the banded silts, levels with dropstones are common. Dropstones include angular to well-rounded clasts of metamorphic rocks (e.g., gneiss, amphibolite, garnet amphibolite), and angular clasts of carbonate rocks from the local rock substrate (Fig. 5A and C). At a few

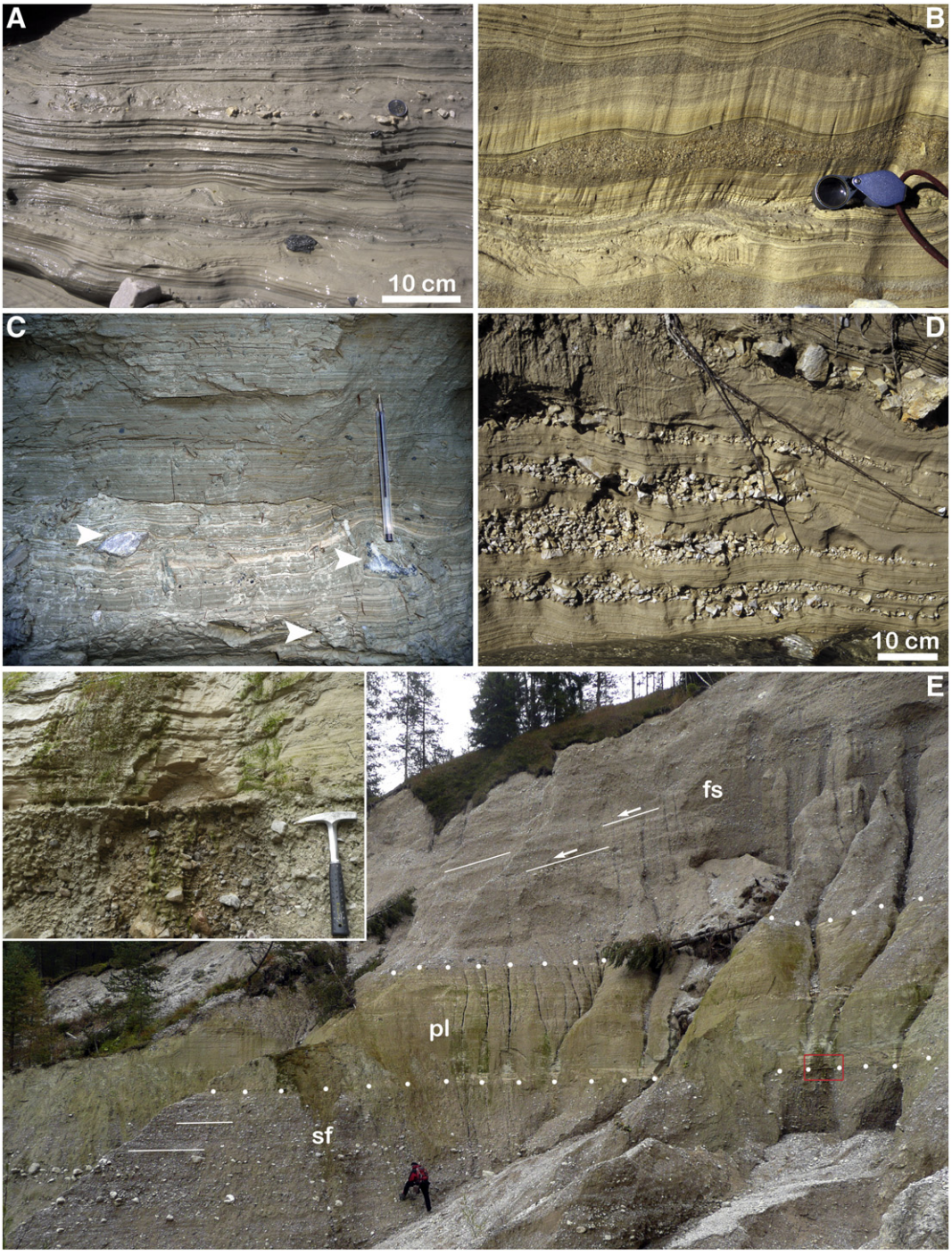

Fig. 5. Quaternary deposits comprising the fill of inner bedrock gorges. (A) Banded silt with isolated dropstones and dropstone 'trails'. (B) Banded silt with intercalated, ripple-drift laminated sandy layers showing pinch-and-swell bedding. Field lens for scale. (C) Banded muddy silt with dropstones (arrow tips) with faceted and polished surfaces. Pencil for scale. (D) Banded silt with intercalated, stacked lenses of gravels to cobbles derived from an adjacent paleocliff (red asterisk in Fig. 8C). (E) Lower part of section B (see Fig. 4), view to southwest. Person stands on gravelly sheet-flow (sf) deposits that are overlain by an interval of banded silts (pl) with dropstones. Up-section, the lacustrine silts interfinger with and are overlain by the foreset (fs) of a Gilbert-type delta. Red rectangle indicates location of inset photo. Inset: Detail of sharp contact between gravelly sheet-flow deposits and overlying banded silts.

locations, unidirectional ripple-drift foreset laminasets of medium to coarse sand are intercalated (Fig. 5B). Banded silts adjacent to and that onlap vertical flanks of pre-glacial bedrock canyons may contain stacked lenses of angular clasts derived from the paleocliff above (Fig. 5D). The banded silts are vertically associated with (i) moderately steeply dipping bedsets of gravelly sand to sandy gravels (foreset beds), and (ii) parallel-horizontally stratified sandy gravels to cobbles (topset beds). As mentioned, the distribution of banded silts versus topset–foreset beds, respectively, indicates that net lacustrine aggradation was punctuated at least once by lake-level lowering and stream incision, followed by renewed lake deposition. The pre-LGM bedrock canyons were mainly filled up by the described proglacial fluviolacustrine succession that is well mappable and exposed in impressive outcrops together with the flanks of buried bedrock gorges (see below).

In contrast to the proglacial succession, outcrops of in situ preserved basal till of the LGM are comparatively rare (Wischounig, 2006; Gruber et al., 2011b). In the environs of Steinberg village, index clasts of metamorphic rocks brought by the Inn ice stream are widespread, but good exposures of till are scarce. In the catchments of Grundache and Gaismoosbach, clasts of metamorphic rocks including Inn-glacier index clasts are comparatively uncommon. This may result from (i) relatively late transfluence of Inn-glacier ice from the West over Kögljoch, and/or (ii) northward flow of local-sourced ice from cirques along the northern face of Rofan massif, combined with (iii) a position of the Grundache–Gaismoos catchments in the lee of overall ice flow (cf. Fig. 2) (Gruber et al., 2011b).

Deposits of the deglacial to early post-glacial interval include resedimented till, kames mainly of proximal-fluvial sediments, and deposits of cohesive debris flows. In cirques along the northern slope of the Rofan massif, moraines of late-Glacial local glaciers, and small rock glaciers to protalus ramparts are present. Furthermore, alluvial fans and scree slopes are common elements of post-glacial sedimentation. Because of scarcity of outcrops, the *relative* amount of post-LGM deposits is not well-constrained everywhere. We assume that ice-marginal, paraglacially redeposited till and remnants of paraglacial, ice-marginal fluviolacustrine deposits are more common as suggested by their rare exposures. Because potential paraglacial deposits are mainly located on mountain slopes today covered by forest and pasture, however, their correct extent is difficult to estimate. Where ice-marginal deposits comprise distinct landforms, such as kames terraces, however, they are readily identified (Gruber et al., 2011b). The extent of talus slopes, alluvial fans, and post-glacial proximal fluvial deposits can be well constrained by a combination of laserscan imagery and outcrops.

5. Steinberger Ache catchment

5.1. Longitudinal profile

Besides an overall concave-up shape, the present longitudinal profile along Grundache–Steinberger Ache is characterized by knickpoints (Fig. 6). In the proximal part of Grundache, knickpoints associated with bedrock channels are present that do not show evidence for slot–canyon cutting (yellow reaches in Fig. 6). Downstream thereof, ten slot canyons of diverse depths and lengths were identified (red reaches in Fig. 6). To temper bedload transport during the twentieth century, the stream was regulated by concrete dams each a few meters in height. The dams were designed to attain a quasibalance between aggradation and erosion along the stream (Josef Plank, Austrian Service of Torrent and Avalanche Control, personal communication, 2011). Along the stream profile, three sharp and comparatively high knicks are associated with post-glacial bedrock slot canyons (Fig. 6).

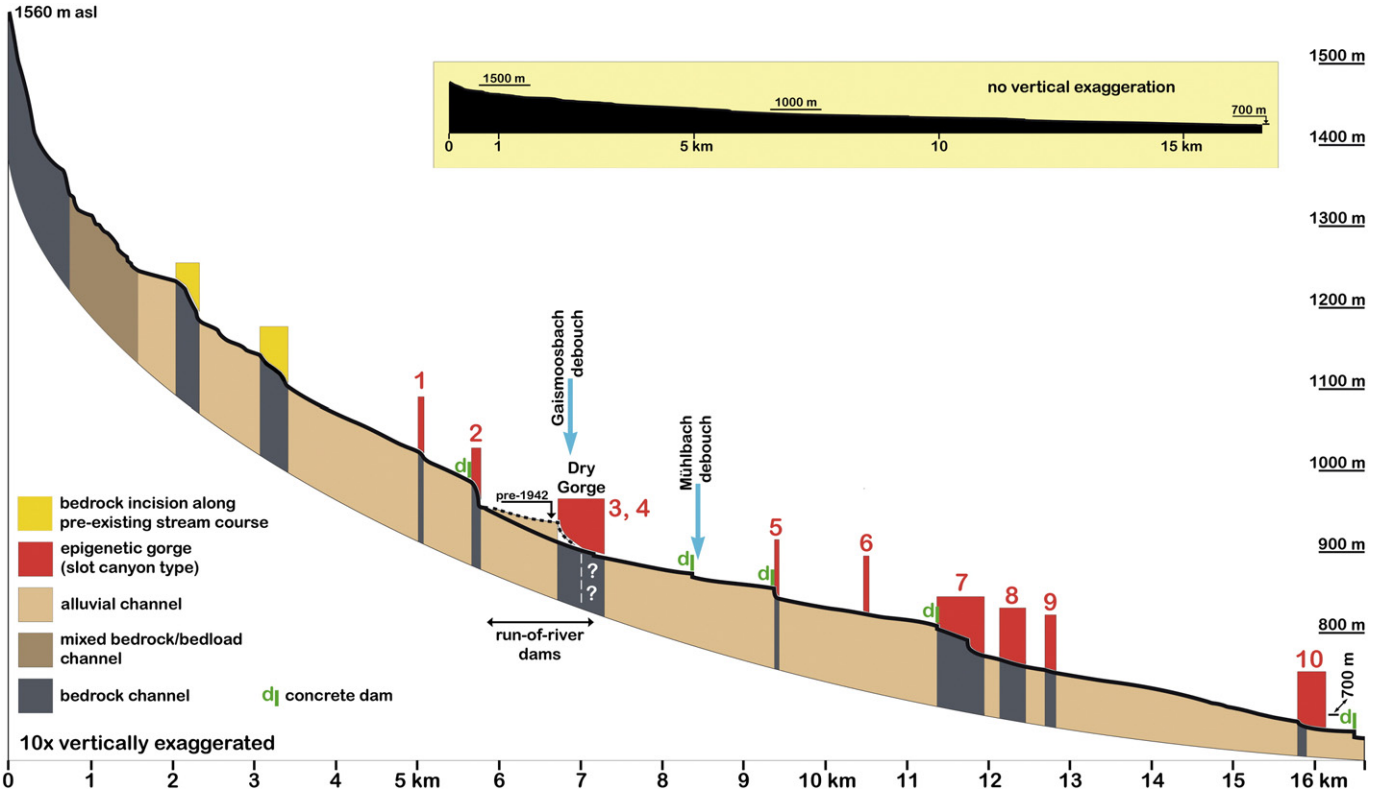

Fig. 6. Longitudinal profile along Grundache–Steinberger Ache (cf. Fig. 2C) showing bedrock and bedload channel reaches and knicks associated with slot canyons. To dampen bedload transport, Steinberger Ache and Grundache have been regulated by dams. Slot canyons are shown with red bars labeled with numbers. In the area of Dry Gorge (slot canyon #3), the natural or pre-1941 stream course (dashed line) has been changed anthropogenically (see text). Upstream of slot canyon #1, the stream bed shows a strongly undulating slope; in this uppermost part of Grundache, the significance of bedrock versus bedload channels, respectively, is difficult to assess.

5.2. Anthropogenic change of stream course

Up to 1941, in the area of their present-day confluence (area 4 in Figs. 2 and 6; section D in Fig. 4), the courses of Gaismoosbach and of Grundache were laterally separated by a natural ridge. This ridge represented an erosional remnant of the proglacial fluviolacustrine succession that had formerly clogged all of Grundache valley. The cross-gorge ridge formed upon post-glacial downcutting of Grundache that deviated from its pre-LGM stream course. This deviation from the older stream course led to the incision of a narrow slot canyon (canyon #4 in Figs. 2C, 4 and 6) that strongly impeded the drift of wood logs. The natural, pre-1941 stream pattern in this area was first documented in a map on a scale of 1: 28,000 of 1801/1805 (Fig. 7A). Several later maps (1816/1821; 1823; 1870/1873) similarly show that Grundache and Gaismoosbach were separated by a narrow ridge (see http://tiris.tirol.gv.at/). In 1940–41, the cross-gorge ridge was removed by blasting (Fig. 7B). Contrary to expectation of planners, the ridge was not cored by rock (Wagner, 1958) but consisted of partly lithified Quaternary sediments (topset deposits of aggrading, proglacial braided-stream stage of Grundache) — unintentionally, the removal of the ridge exposed a buried reach of the pre-LGM Grundache bedrock gorge (Fig. 7B). The U.S. Army map of 1952 first showed the anthropogenically modified course of Grundache (Fig. 7C). After removal of the ridge, Grundache rapidly incised headward into the proglacial deposits (Fig. 7B) that had still partly filled its upstream course (up to epigenesis 2; see Figs. 6 and 8); in the reach downstream thereof, the newly combined waters of Grundache and Gaismoosbach similarly rapidly incised into older sediments.

To manage strongly increased bedload transport because of rejuvenated fluvial incision, in 1942 a concrete dam 6 m in height was erected at Mühlbach debouch, about 1 km downstream of the entrance to Dry Gorge (see Figs. 2C and 6). This dam, however, proved insufficient to cope with bedload. Finally, from 1959 to 1962, a series of run-of-river dams (cf. Csiki and Rhoads, 2010) each about 1.5–2 m in height was built (Wagner, 1958) that proved successful in tempering pulses of bedload transport. Because of the dams, the present stream beds of the lower reach of Grundache and of the middle reach of Steinberger Ache are higher than their natural, undisturbed beds would be. As outlined below, however, this anthropogenic change of stream bed level is not of a magnitude large enough to detract from the reconstructed, natural development of repeated incision, or deepening, of bedrock gorges.

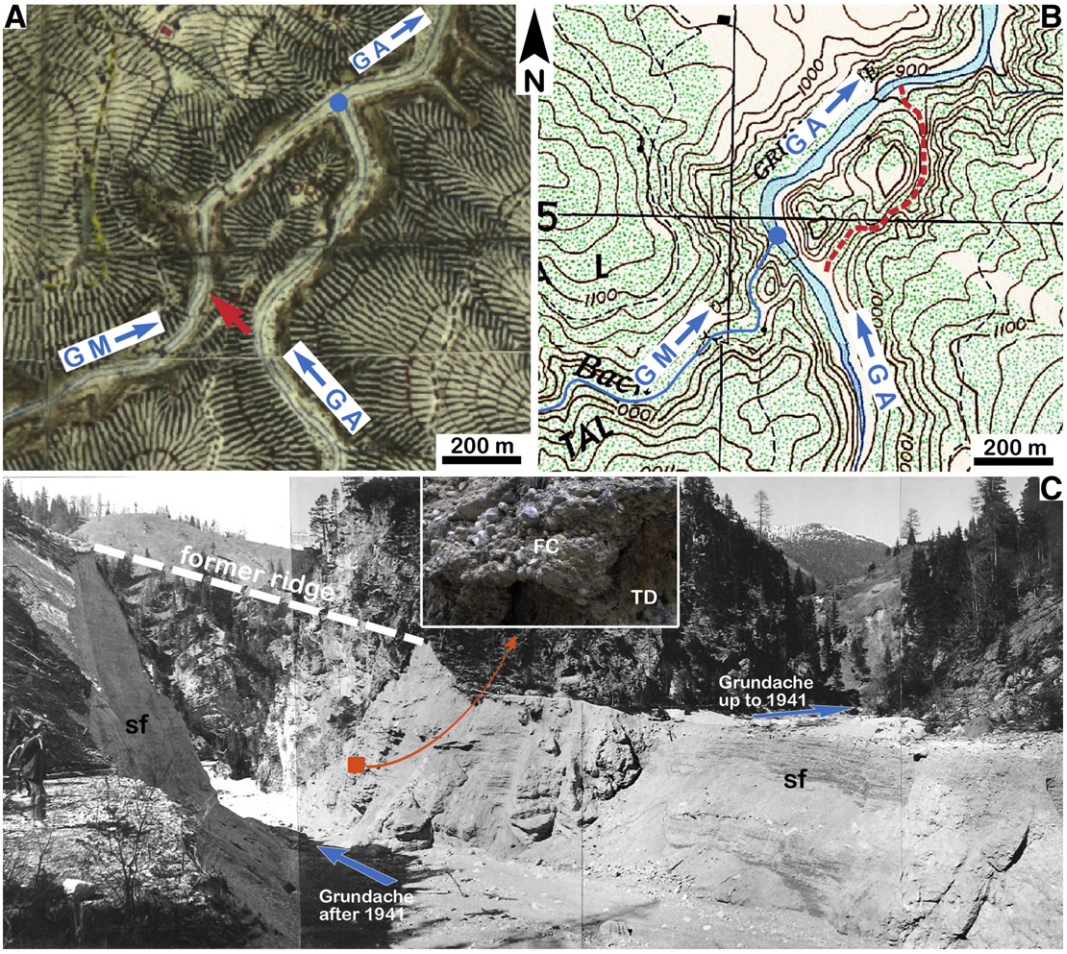

Fig. 7. (A) Map of 1805 showing the confluence of Grundache (GA) and Gaismoosbach (GM) at the debouch of what today is an abandoned, dry bedrock gorge termed Dry Gorge by locals. Red arrow shows location of ridge, removed in 1941, of partly lithified Quaternary deposits. (B) U.S. Army map of 1952 showing stream courses after removal in 1941 of the sediment ridge directly downstream of the former entrance to Dry Gorge. Dashed red line shows course of Grundache up to 1941. (C) Status in 1942 of Grundache canyon in the area of Dry Gorge (area with epigeneses #3 and #4 in Fig. 2C). Erosional incision down to ~10 m of Grundache resulted from blasting away (1941) of a natural ridge across Grundache canyon. Before removal of the ridge, Grundache ran through a post-glacial, epigenetic bedrock gorge. The former cross-valley ridge consisted of partly lithified Quaternary sheet-flow (sf) deposits and, higher up, of proglacial lake deposits (not in photo; see section D in Fig. 4). Shortly before and during the LGM, the fluviolacustrine deposits had completely filled the canyon (see text). Dashed line approximates the crest of the former cross-valley ridge. Photo kindly provided by Josef Plank. Inset photo shows erosional remnant of fluvial conglomerate (FC) onlapping the bedrock canyon wall of Triassic dolostone (TD). For these conglomerates, a U/Th disequilibrium age of cementation of 29.7 ± 1.8 ka is indicated.

5.3. Slot canyons

Along Grundache, the uppermost reach down to ~1.5 km from stream origin consists of bedrock channel and mixed bedrock/bedload channel. Downstream thereof, as mentioned, knickpoints associated with bedrock channels are present that do not show evidence for slot–canyon cutting (yellow reaches in Fig. 6). The first clear-cut epigenetic canyon is present near kilometer 5 of the profile (1 in Fig. 2C, slot canyon #1 in Fig. 6). This canyon consists of a short bedrock gorge with a maximum depth of incision of ~30 m (Fig. 8A and B). Up- and

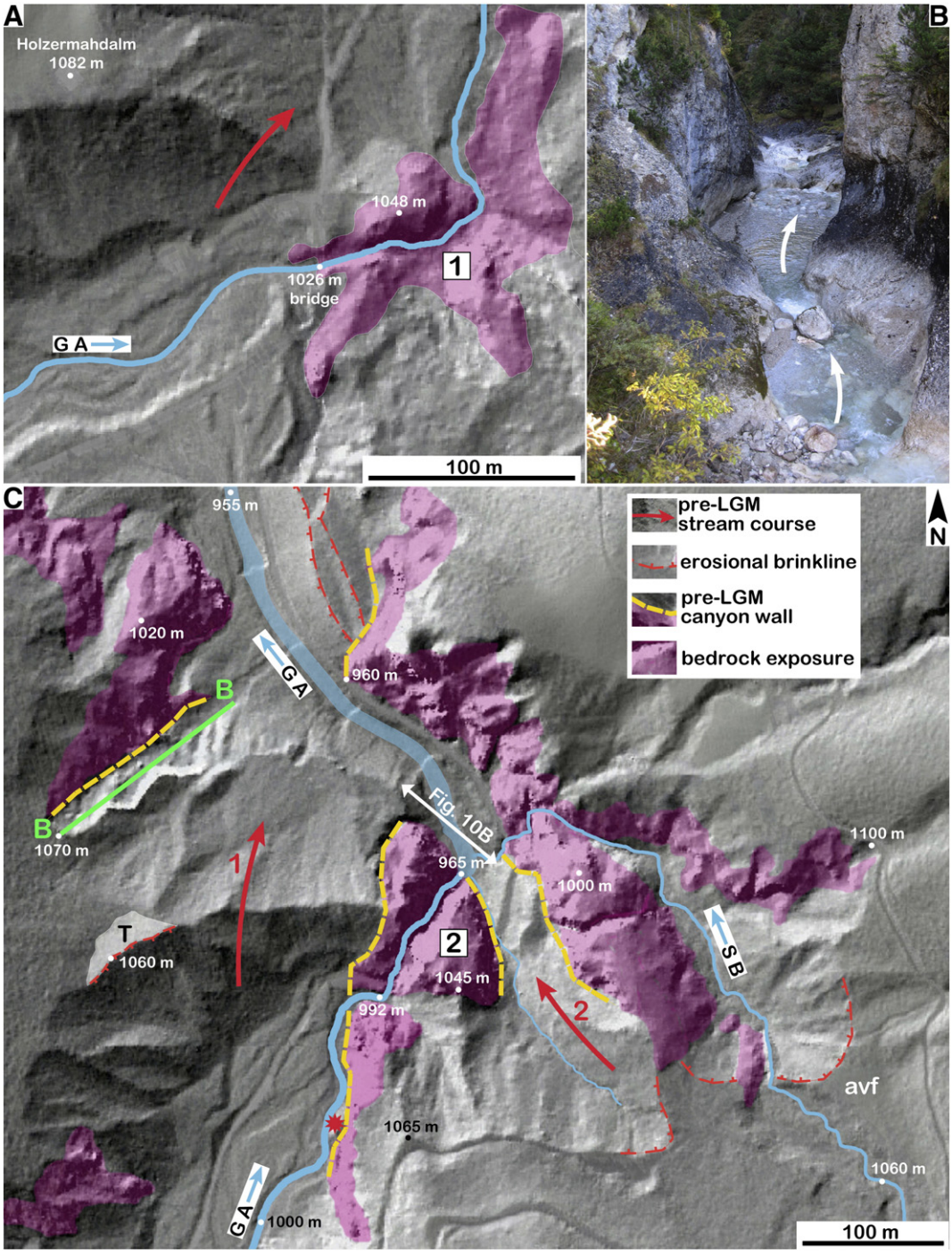

Fig. 8. Map (A) and downstream view (B) of uppermost slot canyon #1 (see Fig. 6). The canyon is incised into Triassic dolostone and is down to 30 m in maximum depth. In subfigure (B), note bedrock channel veneered by gravelly to bouldery sediment at low stage. Red arrow: assumed pre-LGM course of Grundache. (C) Map of slot canyon #2 of Grundache (GA) and epigenetic course of Schauertalbach (SB) (cf. Fig. 2C). Dashed yellow lines indicate walls of pre-LGM bedrock canyons. Red arrow 1: pre-LGM course of Grundache. In this area, the pre-LGM Grundache valley was ~200 m in width and flanked by subvertical bedrock walls (dashed yellow lines; see Fig. 9B). The valley became completely filled with a proglacial fluviolacustrine succession. Green line labeled B denotes section B in Fig. 4 (see also Figs. 5E and 9B). During post-glacial reincision, Grundache cut slot canyon #2 across its former right-hand flank. Along the left bank, a terrace (labeled T) veneered by fluvial gravels rich in clasts of metamorphic rocks (also index clasts of the Inn ice stream) may record a very early stage of post-glacial valley reincision. Red arrow 2: pre-LGM course of Schauertalbach (SB). Also this old canyon was filled up with proglacial fluviolacustrine deposits. During post-glacial reincision, Schauertalbach excavated a short bedrock gully parallel to the buried canyon. Where the gully merges with the flank of the present Grundache canyon, the stream cascades down a waterfall ~35 m in height. Note also erosional brinkline (barbed dashed red line) delimiting the wide, still-aggraded valley floor (avf) of Schauertal Valley.

downstream of this small canyon, Grundache runs within an alluvial channel incised into pre-LGM deposits. Along the banks of Grundache, proglacial lacustrine deposits are locally exposed (Fig. 5A). At one location, the right bank of Grundache consists of a small terrace incised into proglacial lacustrine deposits that onlap a vertical cliff of Triassic carbonate rocks (position marked by asterisk in Fig. 8C). Toward the north, i.e. toward area 2 with epigenetic canyons, the boundary of this rock cliff is continuous in outcrop with the same boundary between bedrock and the proglacial valley fill as exposed in section B (see Figs. 4, 5E, and 9A). The rock cliff that delimits the erosional terrace of proglacial lacustrine deposits thus represents a vestige of the pre-LGM canyon flank. The lacustrine deposits at this location contain stacked, lense-shaped accumulations of angular clasts derived from an adjacent rock cliff (Fig. 5D).

In area 2 (Fig. 2C), the proglacial valley fill and corresponding pre-LGM canyon flanks are spectacularly exposed. Here, the valley fill consists mainly of a package of topset beds that are sharply overlain by lacustrine silts; the latter, in turn, are followed up-section by a package of foreset and topset beds (section B in Figs. 4 and 5E). In addition, the former subvertical canyon flanks onlapped by the proglacial succession are clearly exposed (Figs. 8C and 9B). This indicates that the pre-LGM Grundache ran within an inner bedrock gorge ~200 m in width (arrow 1 in Fig. 8C). The present course of Grundache, in turn, is within a narrow slot canyon (slot canyon #2 in Figs. 6 and 8C). The canyon is characterized by waterfalls and intercalated plunge pools and potholes (Fig. 9A). In area 2, another epigenetic stream reach is present. Today, the small stream Schauertalbach (SB in Figs. 2C, 8C) shows a sharp knick from a relatively low gradient along an aggraded (sediment-filled) valley

Fig. 9. (A) Frontal upstream view into slot canyon #2. Note differentiation into waterfalls and plunge pools. (B) Oblique view onto slot canyon #2 and pre-LGM canyon flank (yellow arrow tips) onlapped by sheet-flow (sf) deposits, proglacial lacustrine (pl) silts, and by the foreset (fs) of a Gilbert-type delta (cf. section B in Figs. 4 and 5E). (C) Downstream view onto knickpoint (red arrow tips) along slot canyon #4 ('Dry Gorge'). At this knick, until 1941, Grundache cascaded down a waterfall about 8 m in height (cf. Fig. 7C). (D) Sky view in the upper part of Dry Gorge. Note narrow gorge width and well-preserved surface of undulating walls. (E) View upstream into the abandoned (since 1941), lower reach of Dry Gorge. Today, the gorge receives only scarce watershed from small brooks cascading down its right flank (white arrows, in background). The gorge is being filled by scree weathering from its flanking cliffs.

above to a bedrock-incised reach downward thereof. The terminal part of Schauertalbach is a waterfall cascading into Grundache (Fig. 8C). The mapped distribution of proglacial deposits and bedrock indicates that the pre-LGM course of Schauertalbach was within a bedrock canyon a few tens of meters in width that today is still clogged by sediments (arrow 2 in Fig. 8C).

Perhaps the most indicative pattern of proglacial valley fills and epigenetic stream reaches is exposed in areas 3 and 4 along Grundache and Gaismoosbach (Fig. 2C). Today, Gaismoosbach drops from an altitude of ~45 m down to the post-1941 level of Grundache (~908 masl; Fig. 10) in a narrow, steep bedrock canyon via waterfalls and intercalated plunge pools and potholes. In addition, the logged distribution of proglacial deposits (section D in Fig. 4) and bedrock indicates that the pre-LGM Gaismoosbach formerly merged with Grundache in a canyon approximately 100 m in width (arrow 1 in Fig. 10). As described, the proglacial deposits comprised a natural ridge, formed by post-glacial erosion, across Grundache canyon (dashed white line in Fig. 10); this ridge was removed in 1941, and Grundache was led back to its pre-LGM course (Fig. 7, see above). The walls of the pre-LGM inner bedrock gorge of Grundache locally still are onlapped by fluvial conglomerates. The $^{234}U/^{230}Th$ disequilibrium dating of isopachous fringes of calcite cement in these conglomerates indicates a precipitation age of 29,694 ± 1770 a (Ostermann, 2006) (Figs. 7B and 10).

As described, the *natural* post-glacial course of Grundache was through a canyon that – subsequent to the anthropogenic change in stream course – was dubbed 'Trockene Klamm' (literally: Dry Gorge) by locals. Dry Gorge can be subdivided into two reaches: (i) an upper 'reach A' with a bedload channel incised into fluvial deposits (Figs. 9B and 10). The most downstream part of reach A is a bedrock channel, abandoned since 1941 – sculpted with longitudinal grooves and potholes – within a bedrock canyon. This channel then sharply knicks off at a waterfall 8 m in height (Fig. 9C; red arrows in Fig. 10). (ii) The waterfall marks the upstream end of 'reach B' of Dry Gorge. The canyon downstream of the waterfall is very narrow and shows undulating cuspate walls sculpted by stream erosion (Fig. 9C and D). In 2001, reach B of the Dry Gorge could be walked out relatively easily back to the former waterfall. In its upstream part, at many locations, reach B showed a well-preserved bedrock channel with undulating walls and with longitudinal grooves, potholes and breached potholes along its base. Rapid deposition of scree derived from the canyon flanks (Fig. 9E) and large

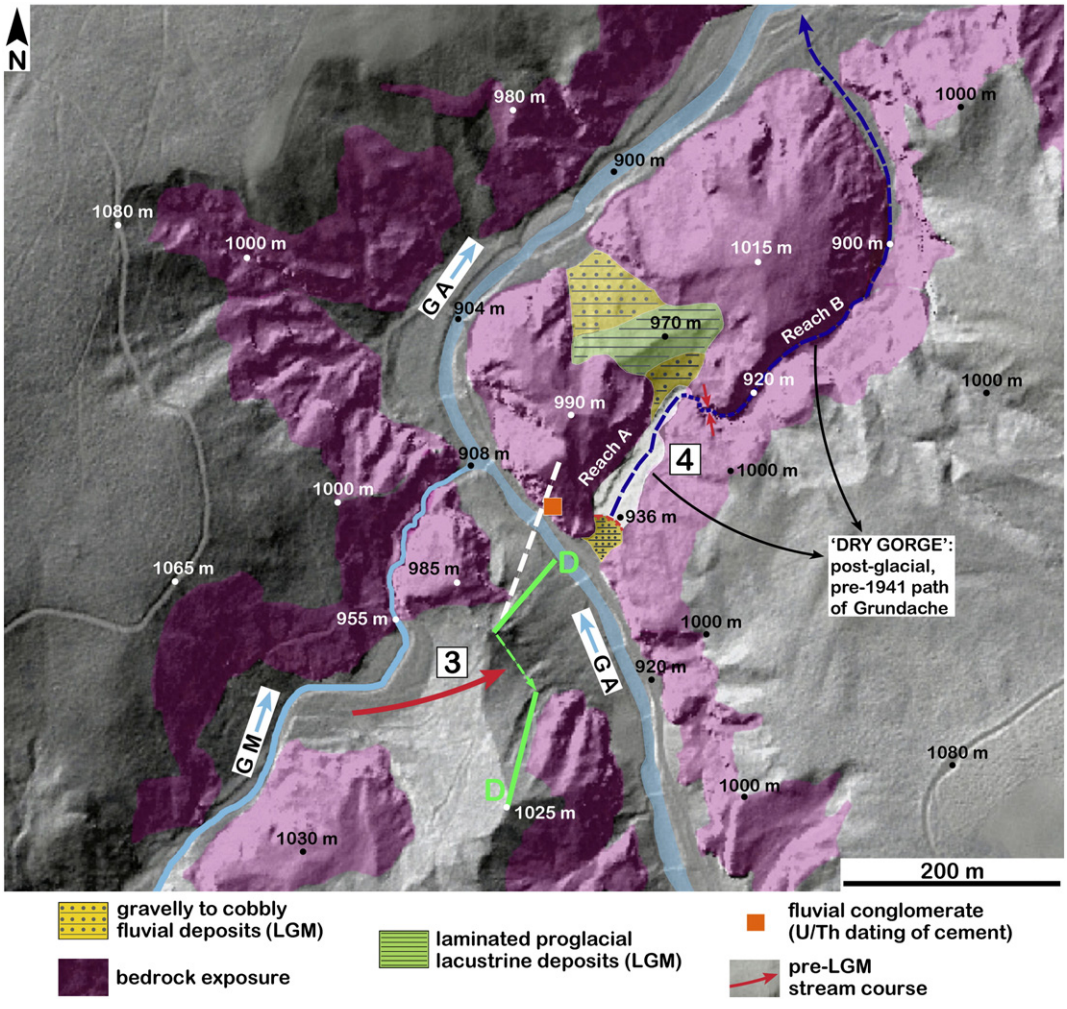

Fig. 10. Map of confluence, at 908 masl, of Grundache (GA) and Gaismoosbach (GM). The present Gaismoosbach descends over a vertical distance of 45 m within a steep slot canyon with waterfalls and plunge pools. Red arrow: pre-LGM course of Gaismoosbach, through a canyon filled by a proglacial fluviolacustrine succession (green line shows trace of section D in Fig. 4). Dashed white line across Grundache valley shows approximated crest of the natural sediment ridge that up to 1941 had separated the post-glacial routes of GM and GA (see Fig. 7A). The ridge consisted of the same fluviolacustrine succession that elsewhere accumulated within the bedrock gorges shortly before the LGM (cf. Figs. 5 and 7). Before anthropogenic removal of the ridge in 1941, Grundache flowed via a bedload channel (reach A, light-gray area) into a narrow bedrock slot canyon (reach B), dubbed Dry Gorge. Red arrows point to a sharp knick with a formerly active waterfall along reach B (see Fig. 9C). Halfway between reaches A and B, note the bedrock canyon filled with the same proglacial succession as elsewhere. Orange quadrangle: fluvial conglomerates onlapping the flank of the pre-LGM Grundache canyon. In this conglomerate, isopachous cement fringes were U/Th-dated to an age of 29.7 ± 1.8 ka (see also Fig. 7C).

rockfalls into the upper part of reach B, however, later made it extremely difficult to pass. The present downstream termination of reach B close to Grundache is a bog.

The bedrock flank along the left side of reach A of Dry Gorge is breached by a short NW-striking canyon ~30 m in width that is filled by the proglacial fluviolacustrine succession (Fig. 10). On the northern end of the sediment-filled canyon, the sediment succession extends down to the present level of Grundache. The surface emergence of bedrock in the lower part of reach A of Dry Gorge and the sharp contrast in canyon width between reaches A and B indicates that reach A connects with the filled breach and is underlain by the proglacial succession over most of its extent (Fig. 11). Together with the clear indications that the present course of Grundache is congruent with its pre-LGM course, this hints on an additional discrete phase of canyon cutting that also preceded the LGM.

Downstream of slot canyon #4, along Steinberger Ache (cf. Fig. 2C), two short slot canyons of a type similar to canyon #1 are present (canyons #5 and #6 in Fig. 6). These are not described in more detail

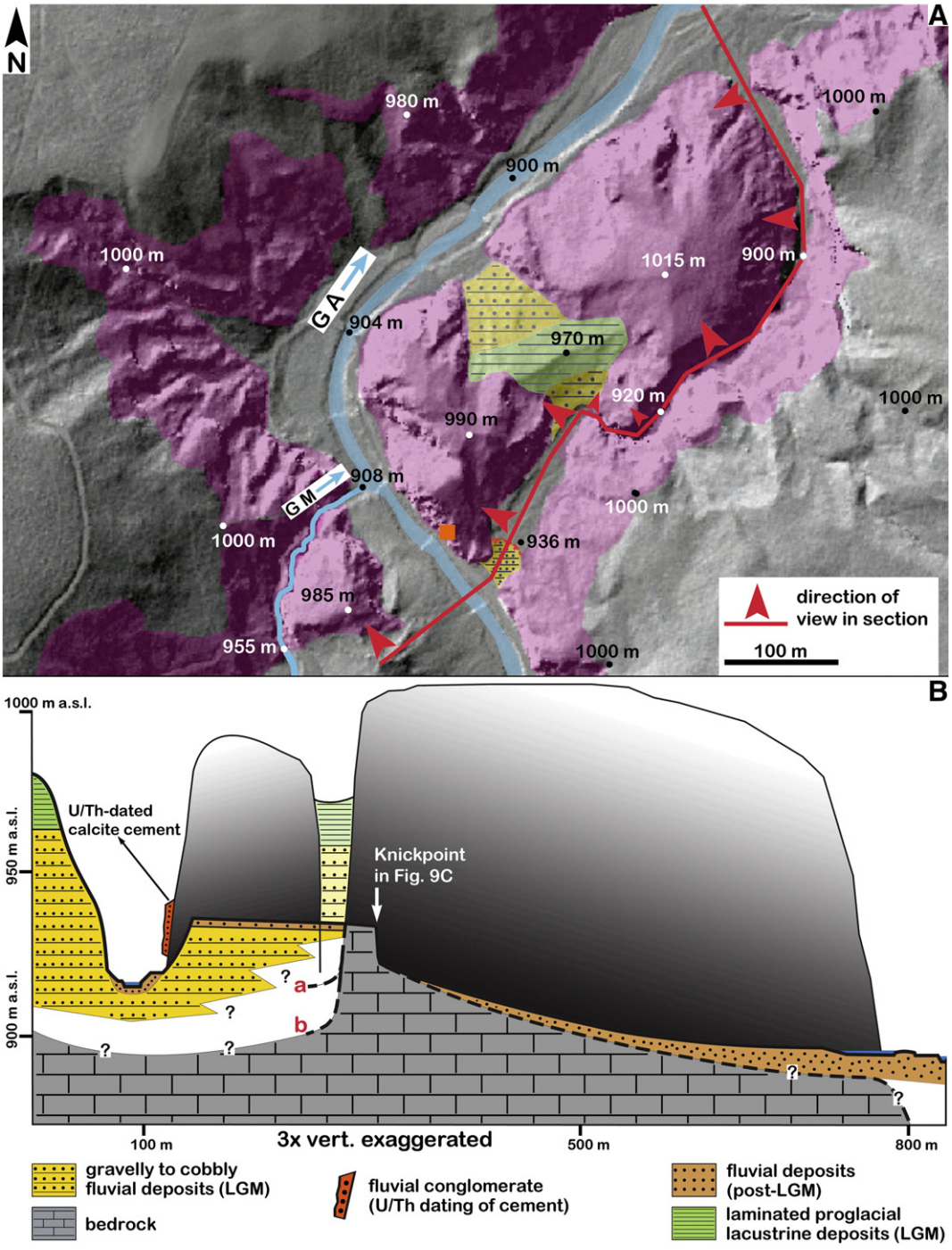

Fig. 11. Plan (A) and schematic section (B) parallel to Dry Gorge, i.e., along the pre-1941 course of Grundache (cf. Fig. 10). The incision of pre-1941 Grundache was anthropogenically halted at a bedrock knick with a formerly active waterfall (Fig. 9C). This knick had laterally receded from a presumed initial position near the right flank of Grundache gorge for more than 500 m; this distance seems fairly large to have formed only by post-LGM incision (see text for discussion). Along the right flank of present Grundache where reach A of Dry Gorge branches off, no bedrock but the succession of fluvial gravels is exposed (see also Fig. 7C). In addition, the two bedrock hills shown shaded-gray are separated by a canyon filled with the same proglacial succession as elsewhere along Grundache. This suggests that the subsurface top of bedrock is located, at least, at the depth of lowest outcrops of the canyon-like breach (line a) or perhaps even deeper (line b). These relations suggest that the sediment-filled canyon and reach A of Dry Gorge are part of a canyon incised before the LGM.

herein. Farther downstream, an array of three slot canyons is present (canyons #7 to #9 in Figs. 2C and 6). In this area directly above the level Steinberger Ache, intervals of fluvial deposits are exposed (Fig. 12A). The fluvial deposits consist exclusively of sand- to cobble-sized clasts derived from the NCA and are sharply overlain by proglacial–lacustrine deposits. In fluvial gravels close to the vertical contact with overlying lacustrine silt, the interstitial pore space is filled by silt. In the area of slot canyons #7–9, the proglacial–lacustrine succession is more than at least 100 m in thickness (Fig. 12A). Each of the slot canyons is floored by bedrock channels (Fig. 6) that, at low stage, contain potholes and grooves littered with gravelly to small-bouldery sediment. In addition, canyon #7 shows a marked knick in profile (Fig. 6) with a waterfall in the gorge. Along the left flank of slot canyon #7, the rock substrate shows an E–W elongate morphological depression down to 820 masl. The depression is filled with lacustrine deposits and, toward the east, is connected with the pre-LGM stream course of Steinberger Ache (Fig. 12A). Two similar, bedrock-incised morphological depressions pinching out a few tens of meters above the present level of Steinberger Ache, and filled with proglacial deposits, were observed farther downstream between slot canyons #9 and #10 (not illustrated). The potential significance of these depressions is discussed farther below.

Closely upstream of the debouch of Steinberger Ache into Brandenberger Ache, another system composed of an active bedrock canyon and an older canyon filled with proglacial–fluvial deposits is present (slot canyon #10 and red arrow in Figs. 2C, 6, and 12B). Upsection from the level of Steinberger Ache, the sediment infill of the canyon starts with a package a few tens of meters thick of subhorizontally stratified fluvial deposits composed exclusively of clasts from the Steinberger Ache catchment. These deposits, in turn, are overlain by

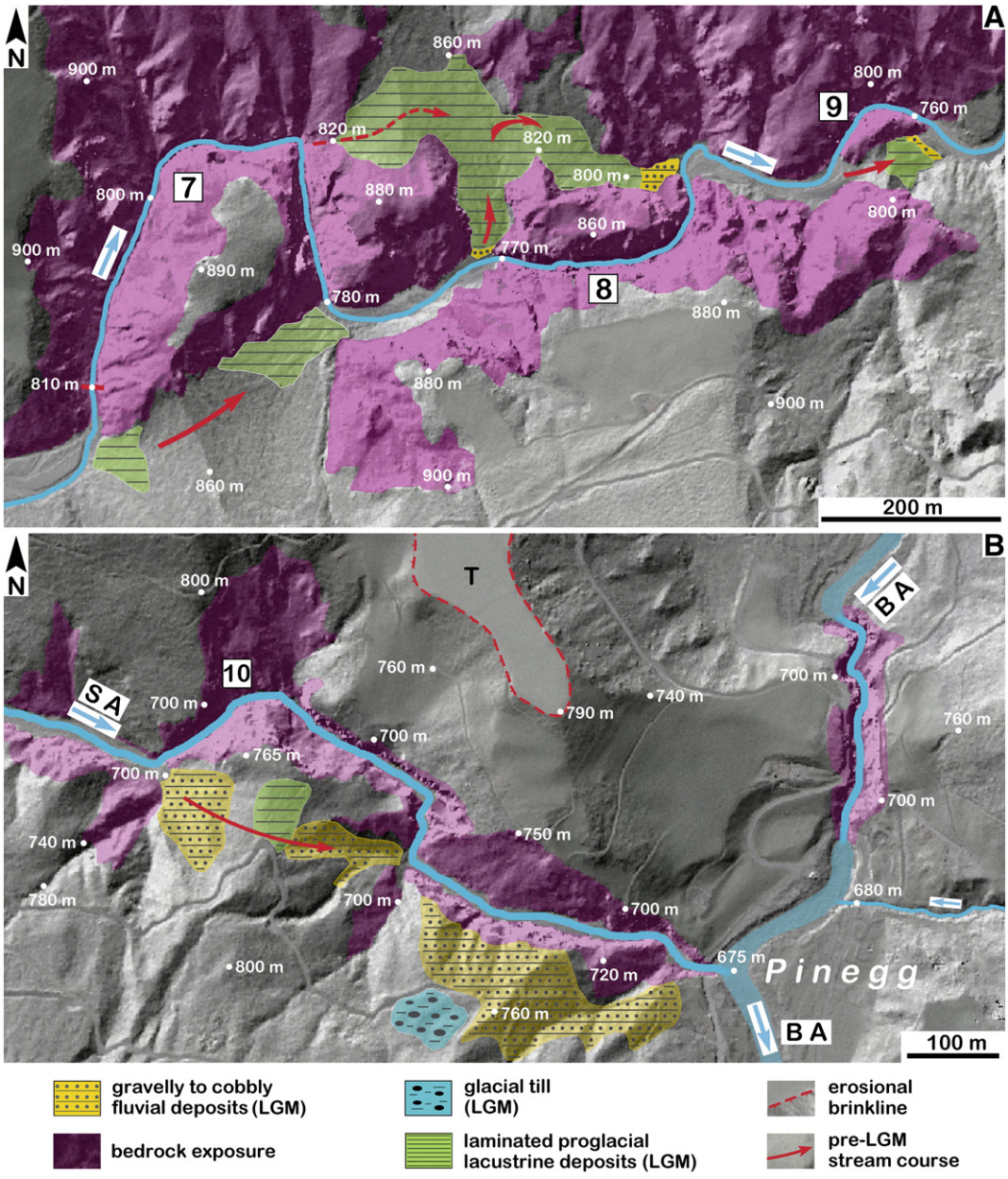

Fig. 12. (A) Succession of slot canyons #7 to #9, middle part of Steinberger Ache (cf. Figs. 2C and 6). Red arrows 1 to 3 indicate the pre-LGM stream course along former canyons that became filled by proglacial fluviolacustrine deposits. The sediment fills within the older canyons indicate that pre-glacial bedrock incision here had attained a similar or larger depth relative to that of the present slot canyons. The bedrock incision indicated with the dashed red arrow at 820 masl might represent a vestige of a still older canyon (see text). (B) Slot canyon #10 (cf. Fig. 6). Note also small slot canyon of Brandenberger Ache adjacent north of Pinegg. Terrace labeled T formed during late-glacial fluvial reincision.

proglacial–lacustrine deposits as described. Locally, the lacustrine deposits are very thin or absent because of erosion along the base of the pleniglacial ice stream (cf. Fig. 2B); at these locations, the fluvial succession is overlain by basal till, or reworked basal till, of the LGM (Fig. 12B).

6. Interpretation and discussion

6.1. Proglacial valley filling

As mentioned in Section 3.2 in the Tyrol, the late phase of MIS 3 was characterized by cool, tundra-like climate associated with marked aggradation of valley floors, presumably between ~36 and 27 ka. The U/Th cementation age of 29,694 ± 1770 a of the fluvial conglomerate of Grundache (cf. Figs. 7B and 9) thus would fit with this phase of valley-bottom sedimentation. Conversely, in the overlying fluviolacustrine succession of Lake Steinberg, the dropstones of metamorphic rocks and the preservation of basal till rich in metamorphic rock fragments still higher above clearly indicate that the lake was in contact with advancing ice streams. The distribution of foreset and topset deposits in the proglacial succession in the area of Gaismoosbach and Grundache (Fig. 4) indicates that the succession contains at least one intraformational unconformity. In proglacial successions resulting from the valley blockade by glaciers, the formation of intrasuccessional unconformities related to intermittent lake outbreaks ('jökulhlaups') is common (e.g., Costa and Schuster, 1988).

6.2. Post-glacial reincision

6.2.1. Potential rates of bedrock incision

Excluding the uppermost 3.4 km of the Grundache–Steinberger Ache system from consideration, the remaining 14.2 km of the stream system contains a total of ~17% of slot canyons (cf. Fig. 6). The present Grundache–Steinberger Ache system thus overlaps fairly well with its pre-glacial precursor. This may be related to glacial erosion being slowed along the lip of the sediment-filled inner bedrock gorges during the pleniglacial phase (cf. Montgomery and Korup, 2011); in addition, the more gently sloping mountain flanks alongside the inner gorges acted to steer post-glacial drainage back to near the former valley axes.

Assuming that the presently active slot canyons all are post-LGM in origin, their vertical depth allows for a rough estimate of required incision rates. For rate estimates, together with Montgomery and Korup (2011, p. 63) we assume that incision started between 15 and 10 ky ago (Fig. 13). Of all the slot canyons, gorges #7 and #8 are deepest; if incised since 15 ky, these canyons required a time-averaged rate of downcutting of 6.7 mm/a. If incised only since 10 ky, a mean incision rate of 10 mm/a was required to arrive at the present depth. For slot canyons #7 and #8, we consider it highly improbable that incision started only during the early Holocene; nevertheless, the figure of 10 mm/a over the last 10 ka can be viewed as a gross uppermost limit for time-averaged, post-glacial, slot-canyon incision in the studied catchment. For the other slot canyons, which are less deeply incised, correspondingly lower rates are required (Fig. 13). To check whether a mean rate of bedrock incision of 10 mm/a over 10 ka can be plausible at all, we had compiled rates of incision documented previously (Table 1). We are aware that many of the incision rates in Table 1 are from areas undergoing surface uplift much more rapidly than that of the present eastern Alps (cf. Höggerl, 2007; Norton and Hampel, 2010). For the sake of a mere comparison of bedrock incision rates, not of tectonic processes and long-term geomorphologic setting, such a comparison can be done. In addition, stream incision is highly episodic, so that longer time intervals are more likely to include phases of little activity and thus show apparently lower rates (cf. Gardner et al., 1987; see Sadler, 1981, 1999, for correlation with respect to sediment accumulation). Higher mean incision rates are documented for intervals of thousands to hundreds of years and correspondingly higher rates for years to months, up to incision in the range of meters during individual floods (Lamb and Fonstad, 2010). With these limitations in mind, it is obvious from Table 1 that a mean incision rate of 10 mm/a over 10 ka is within the range of documented rates over similarly long intervals of time, comprising thousands to ten thousands of years. If excluding a subglacial onset of slot–canyon incision, this supports the hypothesis that the described slot canyons may be even of post-glacial age.

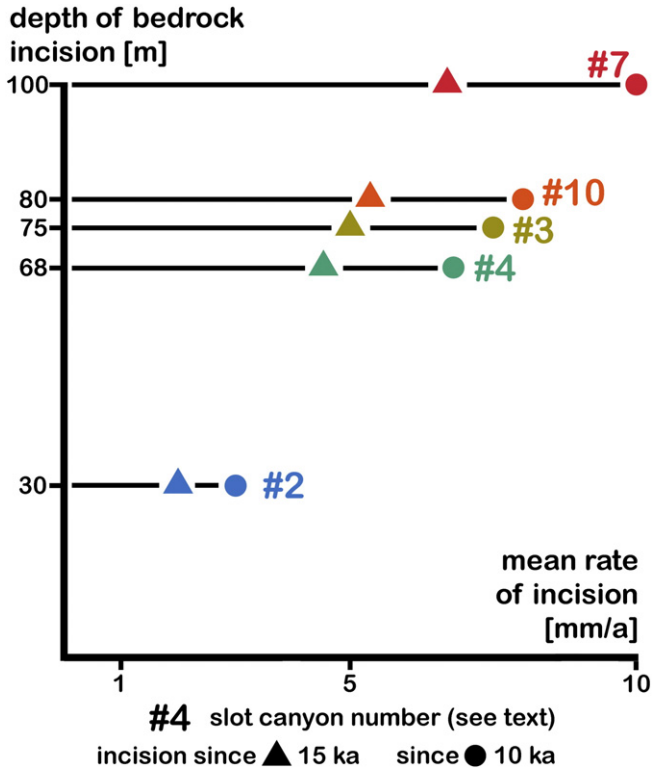

Fig. 13. Diagram to illustrate estimates of required rates of incision of slot canyons. See text for discussion.

At first glance, this conclusion seems to contrast with Montgomery and Korup (2011) who considered a post-LGM incision of entire inner bedrock gorges of the Alps at time-averaged rates of some 8–18 mm/a over 10–15 ky as highly improbable. They argued that the rates of rock exhumation and surface uplift that control the incision of inner bedrock gorges are too low to account for gorge formation solely after the LGM; the inner bedrock gorges of the Alps thus most probably required several major base-level cycles to form (see Montgomery and Korup, 2011). In contrast to entire streams with an inner bedrock gorge, however, slot canyons comprise only a fraction of a stream system and are limited by a local base level determined by the reach directly ahead. The potential rate of slot–canyon cutting thus is largely independent of the processes that control the longer term incision of the entire stream. Because slot–canyon cutting commonly is associated with knickpoints and increased stream power, the erosive capacity of bedload may be higher for short bedrock reaches as it were for an entire catchment. Extremely high rates of slot–canyon incision (Table 1) thus may be related to inherent differences between the excavation of an inner bedrock gorge system over its entire length and the incision of a slot canyon.

6.2.2. Base level of Steinberger Ache

To deduce the pre-LGM base level of Steinberger Ache, knowledge of the subsurface bedrock top and of subsurface Quaternary deposits and their age in the area of Pinegg (cf. Figs. 2C and 12B) was required. Downstream of Pinegg, however, along Brandenberger Ache (Fig. 2C), there is no evidence for major knicks that would indicate a drastic change of base level since before the LGM. Near Brandenberg, an inner bedrock gorge (Tiefenbachklamm, TBK in Fig. 2C) contains erosional remnants

Table 1
Comparative rates of fluvial bedrock incision (arranged according to year of publication).

Item	General information	Rate and time interval	Area	Remarks	Reference
1	Incision of Indus stream into uplifting parts of Himalaya, deduced by exposure dating of strath terraces	2–12 mm/a; total range of rates over time intervals of 6–48 kyr. Max incision ~12 mm/a, averaged over 20 ka (straths 5 to 6; Burbank et al., 1996, their Table 1)	NW Himalaya: Nanga Parbat–Haramosh area	(–)	Burbank et al. (1996)
2	Incision into diverse types of bedrocks, mainly sedimentary rocks	20 mm/a to ~70 mm/a to 100 mm/a, averaged over time periods of up to 300 years. Highest rate: 380 mm/a, observed over period of 2 years	(–)	(–)	Tinkler and Wohl (1998), cited in James (2004, his Table 2, and p. 878)
3	Rate of bedrock incision of Indus stream	Mean rate of 9–12 mm/a over time interval of 7 ka (since 7 ka)	Nanga Parbat–Haramosh area	Rates determined by exposure dating of strath terraces	Leland et al. (1998)
4	Incision into heterolithic succession of marls and sandstones	Rate, calculated for 1912–1999 (87 years): 10–100 mm/a	Alaska, Valley of Tenthousand Smokes	Incision rates based on river diversion by an ash flow in 1912	Whipple et al. (2000)
5	Incision of LiWu stream over 2000 wet season, and 2001 dry + wet seasons	Spatially-averaged rate for quartzite (2000 wet season): 5.5 mm/a; channel base: 1.7 mm/a. Spatially-averaged rate for schist (2000 wet season): 2.3 mm/a; channel base: 0.3 mm/a Total range from 2000 wet season: zero mm/a to 116 m/a. Total range from 2001 dry + wet season: zero to 29.9 mm/a	Eastern coastal range of Taiwan	(–)	Hartshorn et al. (2002)
6	Rate of bedrock incision since the mid-Holocene	Average: 5.1 mm/a (Gori Ganga valley), averaged over time interval since mid-Holocene. High-end rates: 6.6–15.9 mm/a (since mid-Holocene, 4.8–3.3 ka)	Garhwal Himalaya, Nanda Devi region	(–)	Barnard et al. (2004)
7	Slot–canyon cutting (bedrock spur cutoff) resulting from stream diversion by gold-mine tailings (1853–1884)	Mean rate of 250 mm/a, time-averaged from 1894 to 1985. Initial (1884–1890) rates of bedrock incision up to 500 mm/a	Sierra Nevada, western USA	Incision into jointed argillite	James (2004)
8	Rate of bedrock incision at 'time scale' of about 10 ka, deduced from ^{10}Be and ^{26}Al exposure ages of strath surfaces	1.5 mm/a (Mahabarat Range) 7 mm/a (Greater Himalaya)	Nepal Himalaya	(–)	Pratt-Sitaula et al. (2004)
9	Gorge incision in orogenic belt undergoing uplift	Maximum average rate: 26 ± 3 mm/a of gorge incision over middle and late Holocene	Central Range of Taiwan, catchment of LiWu river	(–)	Schaller et al. (2005)
10	Incision along canyons of highly different erodability, based on erosion pins placed into bedrock	Mean local short-term (observation time 1 year to 4.1 years) erosion rates: zero mm/a up to ≥160 mm/a (up to decimeters/a; Stock et al., 2005, p. 193)	Taiwan, Washington, California, Oregon	Geologically 'sustainable' long-term rates are estimated between 0.03 and 1 mm/a	Stock et al. (2005)
11	Minimum rate of incision into bedrock, based on radiocarbon dating of a rockslide event	Minimum rate of stream incision into gneiss over 5.4 ka: 13 mm/a (initial rate probably was much higher; see Pratt-Sitaula et al., 2007)	Marsyandi River, central Nepal	(–)	Pratt-Sitaula et al. (2007)
12	Slot–canyon incision into granite, due to stream diversion by landslide	13 ± 1 mm/a over 3.8 ± 0.3 ka duration (time-averaged minimum incision rate)	Li Qui River, western Sichuan	(–)	Ouimet et al. (2008)
13	Incision of a segment of Braldu River	Seven incision rates, determined by exposure dating of strath terraces. Mean incision rates since 0.9 ± 0.1 ka to 1.2 ± 0.1 ka (three values): 22.9–29.0 mm/a. Mean incision rates since 9.0 ± 0.4 ka to 10.8 ± 0.3 ka (four values): 2.0–3.3 mm/a	Central Karakoram, Pakistan. Along investigated stream segment: succession of gneiss, batholiths and metasediments	Incision probably enhanced by post-glacial uplift above the Main Karakoram Thrust	Seong et al. (2008)
14	Incision into granite, volcanic rocks and sandstone, determined by exposure ages	2.6 ± 1.5 mm/a, over 1.9 ka 0.6 ± 0.1 mm/a, over 9.9 ka 2.4 ± 0.9 mm/a, over 2.47 ka 5.7 ± 2.3 mm/a, over 1.08 ka	Jalisco Block, western Mexico	Jalisco Block is subject to uplift above the active subduction zone of the Pacific Plate	Righter et al. (2010)

of fluvial sands and gravels rich in clasts of metamorphic rocks; these deposits accumulated shortly before the LGM, ahead of the branch of an ice stream that advanced northward along Brandenberg valley (Schreiber, 1949). A precursor of Tiefenbachklamm thus was present before the LGM. The deepest, innermost part with a depth of some 15–20 m of Tiefenbachklamm, however, most probably was excavated by post-LGM incision; this is suggested by narrow width (few meters to ~10 m) of the gorge combined with undulating, cuspate walls sculpted by stream erosion (cf., e.g., Wohl et al., 1999; Schaller et al., 2005). The excavation of the inner gorge of Tiefenbachklamm may be related to (i) incision because of increased watershed area from stream capture associated with breaching of the bedrock canyon Kaiserklamm (a in Fig. 2C); (ii) subglacial stream erosion; and (iii) incision related to differential post-LGM surface uplift. The enhanced watershed by addition of drainage areas north of Kaiserklamm probably increased the potential rate of incision but was not decisive for incision itself; as obvious from the slot canyons along Steinberger Ache, tributary to Brandenberger Ache, the latter has enough watershed to be capable for inner-gorge incision also in the absence of the drainage area north of Kaiserklamm. This is supported by inner bedrock gorges excavated by other streams of the NCA debouching into the left bank of Inn River and by having significantly smaller drainage areas than Brandenberger Ache. Whereas part of the inner-gorge incision may result from subglacial drainage mainly during post-LGM ice decay, we assume that another part of the incision is related to differential surface uplift. For the considered area, a modeled post-LGM (21 ka to present) isostatic surface uplift of, roughly, 40–50 m at Pinegg to 70–80 m near Kramsach (cf. Norton and Hampel, 2010) resulted in a differential uplift of some 20–40 m downstream of Brandenberger Ache. Over time, the uplift decreased exponentially in rate, and present surface uplift in the study area is less than a millimeter per year (Höggerl, 2007). Part of the post-glacial incision of Tiefenbachklamm thus may result from southward-increasing surface uplift after the LGM. In summary, we infer that the pre-LGM base level of Steinberger Ache was positioned at a *grossly* similar altitude (within a few tens of meters) than at present. Along the Grundache–Steinberger Ache system, the knickpoints associated with active slot canyons do not necessarily indicate a lowered base level of the entire catchment; whereas some of the slot canyons take a shorter course than the pre-LGM precursor canyons, others follow a longer route in planview yet may contain knickpoints (e.g., slot canyon #7; Fig. 12A).

6.3. History of canyon incision

The system of presently active slot canyons is causally related to local base-level rise and fall associated with the last glacial–interglacial cycle (incision phase 3 in Fig. 14). Furthermore, the canyon reaches filled with proglacial deposits must have been incised earlier (incision phase 2 in Fig. 14). The sheer width of both sediment-filled and reactivated inner bedrock gorge reaches suggests that these formed over several cycles of base-level rise and fall. In the area of epigenesis #4, the 'surplus' canyon filled with proglacial deposits (red line in Fig. 14, see also Figs. 10 and 11) does not fit well with a simple two-cycle history of base-level rise and fall to explain the origin of the entire canyon system. This situation may be interpreted in two ways: (i) the short reach of a canyon that became filled by proglacial–lacustrine deposits was part of the pre-LGM Grundache canyon, whereas the presently active, curved reach Grundache canyon became incised only after

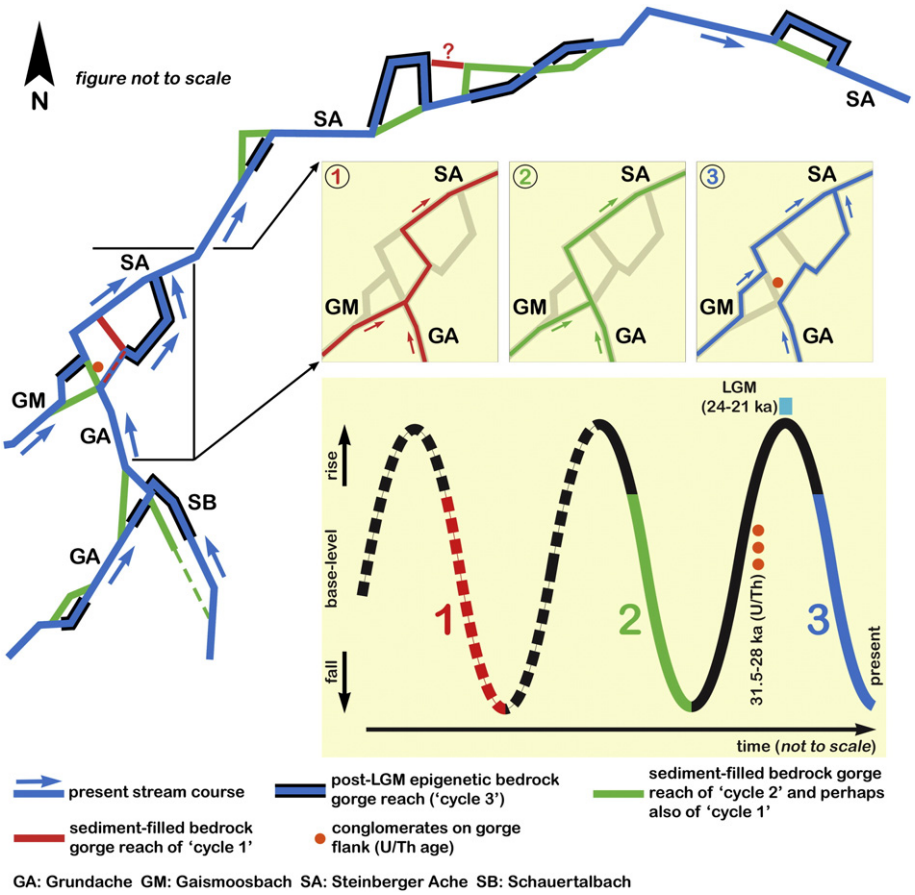

Fig. 14. Summary scheme of stream courses, epigenetic canyons, and relative age of canyon reaches. Stream pattern at Dry Gorge is shown in its pre-1941, natural state. Upper inset Figs. 1 to 3 show hypothetical development of stream network in the area of Dry Gorge. Lower inset figure: possible relation of phases of stream incision to major base-level changes, probably mainly related to glacial–interglacial cycles. See text for discussion.

the last glaciation. We reject this hypothesis, however, for two reasons. First, the curved reach of Grundache canyon is of the same width and shape than its adjacent bedrock reaches; if the curved reach were only of post-LGM age but the adjacent reaches older, then the younger reach should be much more narrow (in analogy to Trockene Klamm and to Grundache waterfall). Second, recall that in this area the fluvial deposits cemented onto the gorge flank and the U/Th conglomerate cementation age indicated that this flank was already in existence before the LGM (see Figs. 10 and 11). Thus, (ii) the short, infilled canyon reach more probably is a vestige of a drainage system older than the LGM, and an additional base-level cycle is required to explain the canyons at epigenesis #4 (incision phase 1 in Fig. 14). As described in the area of epigeneses #7–9 and downstream thereof, morphological bedrock depressions perched with their bases tens of meters above the present stream level might represent vestiges of a still older stream course (cf. Fig. 12). Whether this speculative old stream course correlates with the 'surplus' canyon at epigenesis #4, however, is unknown. Our observations indicate a multicyclic origin of the inner bedrock gorge system of the Steinberger Ache catchment. In essence, the present canyon system consists of aligned reaches of different ages, interspersed with fossil canyons that are filled, entirely or partly still, by late Würmian valley-bottom sediments and/or by proglacial deposits related to the LGM.

6.4. Significance for development of bedrock gorges

That at least most of the inner bedrock gorges of the Alps formed by stream incision over several cycles of major base-level change are now indicated by two independent approaches: (i) the approach of Montgomery and Korup (2011) based on rates of rock exhumation and surface uplift, mentioned above, and (ii) the approach described herein based on a combination of geological mapping with U/Th-dating of the calcite cement of a sedimentary gorge fill. The present course of Grundache and Steinberger Ache essentially is an alignment of inner gorge reaches of markedly different ages, intercalated with abandoned reaches filled with sediment (Fig. 14). To date, old canyons filled with sediments and associated active slot canyons are not indicated in geological maps; this makes these features appear much more rare than they actually are. Further observations by us based mainly on laserscan imagery and field mapping indicate that epigenetic canyons and abandoned gorge reaches are much more common than recognized previously. We suggest sediment-filled valley reaches and slot canyons to be indicated in geological maps, as these features can be labeled with few additional symbols required.

Bedrock-incised stream systems tend to be robust and may be changed, either by rapid and marked base-level changes and/or upon rapid tectonic deformation (e.g., Brocard et al., 2011). In the Alps and similar mountain ranges, base-level changes associated with glacial–interglacial cycles perhaps are the most common trigger of slot canyon development. Additional types of slot canyons include (i) gorges cut in association with subglacial or supraglacial runoff, and (ii) slot canyons formed in response to rapid mass wasting. The different processes that may result in slot canyon formation are not mutually exclusive (e.g., Knauer, 1952; Korup et al., 2006; Ouimet et al., 2007; Pratt-Sitaula et al., 2007; Hewitt et al., 2008; Ouimet et al., 2008). To close, our observations support the conclusion of Montgomery and Korup (2011) that most of the inner bedrock gorges of the Alps formed over several cycles of major base-level change. In addition, our data show that a single inner bedrock gorge may consist of reaches of highly different ages, comprising several cycles of major base-level change.

7. Conclusions

In the catchment of Steinberger Ache river (eastern Alps), the trunk stream and its tributaries comprise a system of bedrock gorges. Each stream course consists of different reaches, including (i) inner bedrock gorges that are up to 200 m in width, changing downstream with (ii) narrow slot canyons. In addition, abandoned bedrock canyons filled with a proglacial fluviolacustrine succession are exposed in large outcrops alongside the active streams. The long-term development of this canyon system was constrained by geological and geomorphological field mapping, facies analysis, and U/Th dating of cements in fluvial deposits.

The proglacial fluviolacustrine succession accumulated during build-up of the Last Glacial Maximum (LGM), when the trunk valley was blocked by advancing ice streams. The proglacial succession aggraded sufficiently high to level out and bury the entire preexisting canyon system. During the LGM, the stream catchment and its sediment-filled canyons were overridden by an ice stream. Upon deglacial ice decay, the drainage system reestablished. Over most of their extent, the downcutting streams reoccupied their pre-glacial inner bedrock canyons in reaming out the proglacial sediment fill. Locally, however, the course of pre-glacial bedrock canyons was 'missed', and post-glacial slot canyons were incised. During reincision of streams, the old abandoned canyon reaches filled with the proglacial succession became well exposed.

In the Alps, systems of inner bedrock gorges and slot canyons resulting from marked base-level rise upon sediment aggradation ahead of the last-Glacial ice streams are widespread. In the Steinberger Ache catchment, however, the mapped distribution of Pleistocene deposits combined with the pattern of canyon incision and a U/Th age of 29.7 ± 1.8 ka of cements in proglacial–fluvial deposits (filling a canyon) record a further discrete phase of base-level rise followed by stream incision older than the LGM. Both the age and the cause of this older base-level rise and fall are not clear to us; it might be related to a glacial advance during the Würm cool phase, but well before the LGM. The U/Th cementation age furthermore suggests that the inner bedrock gorge system is substantially older than 30 ka.

Our results provide direct evidence that a canyon system of the Alps was excavated over multiple cycles of base-level change. The present course of Steinberger Ache and its tributaries essentially is a patchwork composed of (i) presently active, watershed canyons of significantly different widths and ages, and (ii) abandoned, sediment-filled canyon reaches that however might become reactivated upon a future cycle of base-level rise and incision. 'Multicyclic' bedrock canyon systems composed of reaches of highly different ages may be common in the Alps and similar mountain ranges subject to glaciations and/or mass wasting.

Supplementary data to this article can be found online at http://dx.doi.org/10.1016/j.geomorph.2014.03.007.

Acknowledgments

The paper benefited from attentive reading and detailed comments of two anonymous reviewers. Richard Marston is thanked for careful editorial work. Josef Plank, Austrian Service for Torrent and Avalanche Control, is thanked for a field discussion and for providing historical records of anthropogenic changes along Grundache–Steinberger Ache. Dirk Van Husen and Jürgen Reitner provided discussions during a joint field excursion in 2011. Waltraud Wertl, formerly at the Institute of Mineralogy, University of Innsbruck, kindly performed quantitative compositional analyses of XRD samples of lacustrine deposits. Financial support from project 16114-N06 of the Austrian Research Foundation is gratefully acknowledged.

References

Ampferer, O., 1905. Aus der geologischen Geschichte des Achensees. Z. Alpenvereins 1–15.

Bader, K., 1979. Exarationstiefen würmzeitlicher und älterer Gletscher in Südbayern (Trennung eisvorbelasteter und nicht eisvorbelasteter Sedimente aufgrund der seismischen Geschwindigkeiten). Eiszeit. Gegenw. 29, 49–61.

Barnard, P.L., Owen, L.A., Sharma, M.C., Finkel, R.C., 2004. Late Quaternary (Holocene) landscape evolution of a monsoon-influenced high Himalayan valley, Gori Ganga, Nanda Devi, NE Garhwal. Geomorphology 61, 91–110.

Bishop, P., 2007. Long-term landscape evolution: linking tectonics and surface processes. Earth Surf. Process. Landf. 32, 329–365.

Bishop, P., Hoey, T.B., Jansen, J.D., Lexartza Artza, I., 2005. Knickpoint recession rate and catchment area: the case of uplifted rivers in eastern Scotland. Earth Surf. Process. Landf. 30, 767–778.

Brocard, G., Teyssier, C., Dunlap, W.J., Authemayou, C., Simon-Labric, T., Cacao-Chiquín, E. N., Gutiérrez-Orrego, A., Morán-Ical, S., 2011. Reorganization of a deeply incised drainage: role of deformation, sedimentation and groundwater flow. Basin Res. 23, 631–651.

Burbank, D.W., Leland, J., Fielding, E., Anderson, R.S., Brozovic, N., Reid, M.R., Duncan, C., 1996. Bedrock incision, rock uplift and threshold hillslopes in the northwestern Himalayas. Nature 379, 505–510.

Church, M., Ryder, J.M., 1972. Paraglacial sedimentation: a consideration of fluvial processes conditioned by glaciation. Geol. Soc. Am. Bull. 83, 3059–3071.

Costa, J.E., Schuster, R.L., 1988. The formation and failure of natural dams. Geol. Soc. Am. Bull. 100, 1054–1068.

Crosby, B.T., Whipple, K.X., 2006. Knickpoint initiation and distribution within fluvial networks: 236 waterfalls in the Waipaoa River, North Island, New Zealand. Geomorphology 82, 16–38.

Csiki, S., Rhoads, B.L., 2010. Hydraulic and geomorphological effects of run-of-river dams. Prog. Phys. Geogr. 34, 755–780.

de Graaff, L.W.S., 1996. The fluvial factor in the evolution of alpine valleys and of ice-marginal topography in Vorarlberg (W-Austria) during the upper Pleistocene and Holocene. Z. Geomorphol. Neue Folge Suppl. 104, 129–159.

Decker, K., Meschede, M., Ring, U., 1993. Fault slip analysis along the northern margin of the eastern Alps (Molasse, Helvetic nappes, North and South Penninic flysch, and the northern calcareous Alps). Tectonophysics 223, 291–312.

Dunkl, I., Kuhlemann, J., Reinecker, J., Frisch, W., 2006. Cenozoic relief evolution of the eastern Alps — constraints from apatite fission track age-provenance of Neogene intramontane sediments. Mitt. Österr. Geol. Ges. 98, 92–105.

Dürst Stucki, M., Schlunegger, F., Christener, F., Otto, J.-C., Götz, J., 2012. Deepening of inner gorges through subglacial meltwater—an example from the UNESCO Entlebuch area, Switzerland. Geomorphology 139–140, 506–517.

Eisbacher, G.H., Brandner, R., 1996. Superposed fold–thrust structures and high-angle faults, northwestern calcareous Alps, Austria. Eclogae Geol. Helv. 89, 553–572.

Fliri, F., Bortenschlager, S., Felber, H., Heissel, W., Hilscher, H., Resch, W., 1970. Der Bänderton von Baumkirchen (Inntal, Tirol). Eine neue Schlüsselstelle zur Kenntnis der Würm-Vereisung der Alpen. Z. Gletscherk. Glazialgeol. 6, 5–35.

Frank, N., Braum, M., Hambach, U., Mangini, A., Wagner, G., 2000. Warm period growth of travertine during the last interglaciation in southern Germany. Quat. Res. 54, 38–48.

Frankel, K.L., Pazzaglia, F.J., Vaughn, J.D., 2007. Knickpoint evolution in a vertically bedded substrate, upstream-dipping terraces, and Atlantic slope bedrock channels. Geol. Soc. Am. Bull. 119, 476–486.

Frisch, W., Kuhlemann, J., Dunkl, I., Brügel, A., 1998. Palinspastic reconstruction and topographic evolution of the eastern Alps during late Tertiary tectonic extrusion. Tectonophysics 297, 1–15.

Frisch, W., Kuhlemann, J., Dunkl, I., Székely, B., 2001. The Dachstein paleosurface and the Augenstein Formation in the northern calcareous Alps — a mosaic stone in the geomorphological evolution of the eastern Alps. Int. J. Earth Sci. 90, 500–518.

Fügenschuh, B., Mancktelow, N., Seward, D., 2000. Cretaceous to Neogene cooling and exhumation history of the Oetztal–Stubai basement complex, eastern Alps: a structural and fission track study. Tectonics 19, 905–918.

Gardner, T.W., 1983. Experimental study of knickpoint and longitudinal profile evolution in cohesive, homogeneous material. Geol. Soc. Am. Bull. 94, 664–672.

Gardner, T.W., Jorgensen, D.W., Shuman, C., Lemieux, C.R., 1987. Geomorphic and tectonic process rates: effects of measured time interval. Geology 15, 259–261.

Geyh, M.A., 2001. Reflections on the ^{230}Th/U dating of dirty material. Geochronometria 20, 9–14.

Geyh, M.A., 2005. Handbuch der physikalischen und chemischen Altersbestimmung. Wissenschaftliche Buchgesellschaft, Darmstadt (211 pp.).

Geyh, M.A., 2008. Selection of suitable data sets improves ^{230}Th/U dates of dirty material. Geochronometria 30, 69–77.

Gruber, A., 2008. Bericht 2006 über geologische Aufnahmen auf den Blättern 88 Achenkirch und 119 Schwaz. Jahrb. Geol. Bundesanst. 148, 277–281.

Gruber, A., 2011. Die neue Geologische Karte "Geologie des nördlichen Achenseeraumes-ÖK Blatt 88 Achenkirch". Einführung und geologische Forschungsgeschichte. In: Gruber, A. (Ed.), Arbeitstagung 2011 der Geologischen Bundesanstalt Blatt 88 Achenkirch. Geological Survey of Austria, Vienna, pp. 5–16.

Gruber, A., Rabeder, J., Wimmer-Frey, I., 2011a. Seetone aus Quartärablagerungen auf Blatt ÖK 88 Achenkirch. In: Gruber, A. (Ed.), Arbeitstagung 2011 der Geologischen Bundesanstalt Blatt 88 Achenkirch. Geological Survey of Austria, Vienna, pp. 121–124.

Gruber, A., Wischounig, L., Sanders, D., 2011b. Ablagerungs- und Flussgeschichte während des späten Quartärs im Bereich nördlich des Rofan. In: Gruber, A. (Ed.), Arbeitstagung 2011 der Geologischen Bundesanstalt Blatt 88 Achenkirch. Geological Survey of Austria, Vienna, pp. 226–246.

Hartshorn, K., Hovius, N., Dade, W.B., Slingerland, R.L., 2002. Climate-driven bedrock incision in an active mountain belt. Science 297, 2036–2038.

Hewitt, K., 2006. Disturbance regime landscapes: mountain drainage systems interrupted by large rockslides. Prog. Phys. Geogr. 30, 365–393.

Hewitt, K., Clague, J.J., Orwin, J.F., 2008. Legacies of catastrophic rock slope failures in mountain landscapes. Earth Sci. Rev. 87, 1–38.

Hirtlreiter, G., 1992. Spät-und postglaziale Gletscherschwankungen im Wettersteingebirge und seiner Umgebung. Münch. Geogr. Abh. Reihe B 15, 154.

Höggerl, N., 2007. Höhenänderungen in Österreich. In: Hofmann, T., Schönlaub, H.P. (Eds.), Geo-Atlas Österreich. Böhlau Print, Vienna, pp. 56–57.

Horvacki, J., 1982. Ablagerungsmodell der Tiroler Bändertone aufgrund sedimentpetrographischer Analysen mit rohstoffkundlicher Bewertung. (Ph.D. thesis) University of Innsbruck, Austria (124 pp.).

Ivy-Ochs, S., Kerschner, H., Kubik, P.W., Schlüchter, C., 2006. Glacier response in the European Alps to Heinrich event I cooling: the Gschnitz stadial. J. Quat. Sci. 21, 115–130.

Ivy-Ochs, S., Kerschner, H., Reuther, A., Preusser, F., Heine, K., Maisch, M., Kubik, P.W., Schlüchter, C., 2008. Chronology of the last glacial cycle in the European Alps. J. Quat. Sci. 23, 559–573.

Ivy-Ochs, S., Kerschner, H., Maisch, M., Christl, M., Kubik, P.W., Schlüchter, C., 2009. Latest Pleistocene and Holocene glacier variations in the European Alps. Quat. Sci. Rev. 28, 2137–2149.

James, L.A., 2004. Tailings fans and valley-spur cutoffs created by hydraulic mining. Earth Surf. Process. Landf. 29, 869–882.

Kaufman, A., Broecker, W.S., 1965. Comparison of ^{230}Th and ^{14}C ages for carbonate materials from lakes Lahontan and Bonneville. J. Geophys. Res. 70, 4039–4054.

Kerschner, H., Hertl, A., Gross, G., Ivy-Ochs, S., Kubik, P.Q., 2006. Surface exposure dating of moraines in the Kromer valley (Silvretta Mountains, Austria) — evidence for glacial response to the 8.2 ka event in the eastern Alps? The Holocene 16, 7–15.

Knauer, J., 1952. Diluviale Talverschüttung und Epigenese im südlichen Bayern. Geol. Bavarica 11, 1–32.

Korup, O., Strom, A., Weidinger, J.T., 2006. Fluvial response to large rock-slope failures: examples from the Himalayas, the Tien Shan, and the Southern Alps in New Zealand. Geomorphology 78, 3–21.

Kuhlemann, J., 2007. Paleogeographic and paleotopographic evolution of the Swiss and eastern Alps since the Oligocene. Glob. Planet. Chang. 58, 224–236.

Kuhlemann, J., Frisch, W., Székely, B., Dunkl, I., Kazmer, M., 2002. Post-collisional sediment budget history of the Alps: tectonic versus climatic control. Int. J. Earth Sci. 91, 818–837.

Kuhlemann, J., Dunkl, I., Bruegel, A., Spiegel, C., Frisch, W., 2006. From source terrains of the eastern Alps to the Molasse basin: detrital record of non-steady-state exhumation. Tectonophysics 413, 301–316.

Lamb, M.P., Fonstad, M.A., 2010. Rapid formation of a modern bedrock canyon by a single flood event. Nat. Geosci. 3, 477–481.

Leland, J., Reid, M.R., Burbank, D.W., Finkel, R., Caffee, M., 1998. Incision and differential bedrock uplift along the Indus River near Nanga Parbat, Pakistan Himalaya, from ^{10}Be and ^{26}Al exposure age dating of bedrock straths. Earth Planet. Sci. Lett. 154, 93–107.

Lin, J.C., Broecker, W.S., Anderson, R.F., Hemming, S., Rubenstone, J.L., Bonani, G., 1996. New ^{230}Th/^{234}U and ^{14}C ages from Lake Lahontan carbonates, Nevada, USA, and a discussion of the origin of initial thorium. Geochim. Cosmochim. Acta 60, 2817–2832.

Linzer, H.-G., Ratschbacher, L., Frisch, W., 1995. Transpressional collision structures in the upper crust: the fold–thrust belt of the northern calcareous Alps. In: Neubauer, F., Wallbrecher, E. (Eds.), Tectonics of the Alpine–Carpathian–Pannonian region. Tectonophysics, 242, pp. 41–61.

Ludwig, K.R., Titterington, D.M., 1994. Calculation of ^{230}Th/^{234}U isochrons, ages, and errors. Geochim. Cosmochim. Acta 58, 5031–5042.

Martinson, D.G., Pisias, N.G., Hays, J.D., Imbrie, J., Moore, T.C., Shackleton, N.J., 1987. Age dating and the orbital theory of the ice ages: development of a high resolution 0 to 300.000-year chronostratigraphy. Quat. Res. 27, 1–29.

Monegato, G., Ravazzi, C., Donegana, M., Pini, R., Calderoni, G., Wick, L., 2007. Evidence of a two-fold glacial advance during the Last Glacial Maximum in the Tagliamento end moraine system (eastern Alps). Quat. Res. 68, 284–302.

Montgomery, D.R., Buffington, J.M., 1997. Channel-reach morphology in mountain drainage basins. Geol. Soc. Am. Bull. 109, 596–611.

Montgomery, D.R., Korup, O., 2011. Preservation of inner gorges through repeated Alpine glaciations. Nat. Geosci. 4, 62–67.

Muttoni, G., Carcano, C., Garzanti, E., Ghielmi, M., Piccin, A., Pini, R., Rogledi, S., Sciunnach, D., 2003. Onset of major Pleistocene glaciations in the Alps. Geology 31, 989–992.

Norton, K.P., Hampel, A., 2010. Postglacial rebound promotes glacial re-advances—a case study from the European Alps. Terra Nova 22, 297–302.

Ortner, H., Stingl, V., 2001. Facies and basin development of the Oligocene in the lower Inn Valley. In: Piller, W., Rasser, M. (Eds.), The Paleogene in Austria. Schriftenreihe der Erdwissenschaftlichen Kommission 14. Österreichische Akademie der Wissenschaften, Wien, pp. 153–196.

Orwin, J.F., Smart, C.C., 2004. The evidence for paraglacial sedimentation and its temporal scale in the deglacierizing basin of Small River Glacier, Canada. Geomorphology 58, 175–202.

Osmond, J.K., May, J.P., Tanner, W.F., 1970. Age of the Cape Kennedy barrier and lagoon complex. J. Geophys. Res. 75, 469–479.

Ostermann, M., 2006. Thorium–Uranium Age-Dating of "Impure" Carbonate Cements of Selected Quaternary Depositional Systems of Western Austria: Results, Implications, Problems. (Ph.D. thesis) University of Innsbruck, Austria (173 pp.).

Ostermann, M., Sanders, D., Kramers, J., 2006. ^{230}Th/^{234}U ages of calcite cements of the proglacial valley fills of Gamperdona and Bürs (Riss Ice Age, Vorarlberg, Austria): geological implications. Aust. J. Earth Sci. 99, 31–41.

Ouimet, W.B., Whipple, K.X., Royden, L.H., Sun, Z., Chen, Z., 2007. The influence of large landslides on river incision in a transient landscape: eastern margin of the Tibetan Plateau (Sichuan, China). Geol. Soc. Am. Bull. 119, 1462–1476.

Ouimet, W.B., Whipple, K.X., Crosby, B.T., Johnson, J.P., Schildgen, T.F., 2008. Epigenetic gorges in fluvial landscapes. Earth Surf. Process. Landf. 33, 1993–2009.

Patzelt, G., 1980. Neue Ergebnisse der Spät- und Postglazialforschung in Tirol. Jahresberichte der Österreichischen Geographischen Gesellschaft, 76/77 11–18.

Penck, A., Brückner, E., 1901/1909. Die Alpen im Eiszeitalter. Tauchnitz, Leipzig (1199 pp.).
Piller, W.E., Egger, H., Erhart, C.W., et al., 2004. Die stratigraphische Tabelle von Österreich 2004 (sedimentäre Schichtfolgen). Gerin print, Wolkersdorf.
Poscher, G., 1994. Fazies und Genese der pleistozänen Terrassensedimente im Tiroler Inntal und seinen Seitentälern-Teil 1: Der Achenseedamm. Jahrb. Geol. Bundesanst. 137, 171–186.
Pratt-Sitaula, B., Burbank, D.W., Heimsath, A., Ojha, T., 2004. Landscape disequilibrium on 1000–10,000 year scales, Marsyandi River, Nepal, central Himalaya. Geomorphology 58, 223–241.
Pratt-Sitaula, B., Garde, M., Burbank, D.W., Oskin, M., Heimsath, A., Gabet, E., 2007. Bedload-to-suspended load ratio and rapid bedrock incision from Himalayan landslide-dam lake record. Quat. Res. 68, 111–120.
Preusser, F., 2004. Towards a chronology of the late Pleistocene in the northern Alpine foreland. Boreas 33, 195–210.
Preusser, F., Reitner, J.M., Schlüchter, C., 2010. Distribution, geometry, age and origin of overdeepened valleys and basins in the Alps and their foreland. Swiss J. Geosci. 103, 407–426.
Ratschbacher, L., Frisch, W., Linzer, H.-G., Merle, O., 1991. Lateral extrusion in the eastern Alps, part 2: structural analysis. Tectonics 10, 257–271.
Reitner, J.M., 2007. Glacial dynamics at the beginning of Termination I in the eastern Alps and their stratigraphic implications. Quat. Int. 164–165, 64–84.
Reitner, J., 2011. Das Inngletschersystem während des Würm-Glazials. In: Gruber, A. (Ed.), Arbeitstagung 2011 der Geologischen Bundesanstalt, Blatt 88 Achenkirch. Geological Survey of Austria, Vienna, pp. 79–88.
Righter, K., Caffee, M., Rosas-Elguera, J., Valencia, V., 2010. Channel incision in the Rio Atenguillo, Jalisco, Mexico, defined by ^{36}Cl measurements of bedrock. Geomorphology 120, 279–292.
Robl, J., Hergarten, S., Stüwe, K., 2008a. Morphological analysis of the drainage system in the eastern Alps. Tectonophysics 460, 263–277.
Robl, J., Stüwe, K., Hergarten, S., Evans, L., 2008b. Extension during continental convergence in the eastern Alps: the influence of orogen-scale strike-slip faults. Geology 36, 963–966.
Rosenberg, C.L., Brun, J.-P., Gapais, D., 2004. Indentation model of the eastern Alps and the origin of the Tauern window. Geology 32, 997–1000.
Rosholt, N., 1976. ^{230}Th/^{234}U dating of travertines and caliche rinds. Geol. Soc. Am. Abstr. Programs 8, 1079.
Sadler, P.M., 1981. Sediment accumulation rates and the completeness of stratigraphic sections. J. Geol. 89, 569–584.
Sadler, P.M., 1999. The influence of hiatuses on sediment accumulation rates. GeoRes. Forum 5, 15–40.
Sanders, D., 2012. Effects of deglacial sedimentation pulse, followed by incision: a case study from a catchment in the northern calcareous Alps (Austria). E&G Quat. Sci. J. 61, 16–31.
Sanders, D., Ostermann, M., 2011. Post-last glacial alluvial fan and talus slope associations (northern calcareous Alps, Austria): a proxy for late Pleistocene to Holocene climate change. Geomorphology 131, 85–97.
Sanders, D., Wischounig, L., Ostermann, M., 2006. Here it hit, there it missed: late Quaternary patterns of deposition and fluvial incision, Steinberg am Rofan (northern calcareous Alps) (abstr.). In: Tessadri-Wackerle, M. (Ed.), Pangeo 2006. Conference Series. Innsbruck University Press, Austria, pp. 299–300.
Schaller, M., Hovius, N., Willett, S.D., Ivy-Ochs, S., Synal, H.-A., Chen, M.-C., 2005. Fluvial bedrock incision in the active mountain belt of Taiwan from in situ-produced cosmogenic nuclides. Earth Surf. Process. Landf. 30, 955–971.
Schmid, S.M., Fügenschuh, B., Kissling, E., Schuster, R., 2004. Tectonic map and overall architecture of the Alpine orogen. Eclogae Geol. Helv. 97, 93–117.
Schreiber, W., 1949. Über die Klammbildung und Talverschüttung im Brandenberg-Steinberger Gebiet. Veröffentlichungen des Tiroler Landesmuseums Ferdinandeum, 26–29, pp. 33–60.
Seidl, M.A., Dietrich, W.E., Kirchner, J.W., 1994. Longitudinal profile development into bedrock: an analysis of Hawaiian channels. J. Geol. 102, 457–474.
Seong, Y.B., Owen, L.A., Bishop, M.P., Bush, A., Clendon, P., Copland, L., Finkel, R.C., Kamp, U., Shroder Jr., J.F., 2008. Rates of fluvial bedrock incision within an actively uplifting orogen: central Karakoram Mountains, northern Pakistan. Geomorphology 97, 274–286.
Severinghaus, J.P., Sowers, T., Brook, E.J., Alley, R.B., Bender, M.L., 1998. Timing of abrupt climate change at the end of the Younger Dryas interval from thermally fractionated gases in polar ice. Nature 391, 141–148.
Starnberger, R., Rodnight, H., Spötl, C., 2011. Chronology of the Last Glacial Maximum in the Salzach Palaeoglacier area (eastern Alps). J. Quat. Sci. 26, 502–510.
Sternai, P., Herman, F., Champagnac, J.-D., Fox, M., Salcher, B., Willett, S.D., 2012. Pre-glacial topography of the European Alps. Geology 40, 1067–1070.
Stock, J.D., Montgomery, D.R., Collins, B.D., Dietrich, W.E., Sklar, L., 2005. Field measurements of incision rates following bedrock exposure: implications for process controls on the long profiles of valleys cut by rivers and debris flows. Geol. Soc. Am. Bull. 117, 174–194.
Tinkler, K.J., Wohl, E.E. (Eds.), 1998. Rivers over rock: Fluvial processes in bedrock channels, 107. American Geophysical Union, Monograph, Washington DC, pp. 1–18.
Tricart, J., 1960. A subglacial gorge: La gorge du Guil (Hautes Alpes). J. Glaciol. 3, 646–651.
Tunnicliffe, J.F., Church, M., 2011. Scale variation of post-glacial sediment yield in Chilliwack Valley, British Columbia. Earth Surf. Process. Landf. 36, 229–243.
Van Husen, D., 1977. Zur Fazies und Stratigraphie der jungpleistozänen Ablagerungen im Trauntal. Jahrb. Geol. Bundesanst. 120, 130.
Van Husen, D., 1979. Verbreitung, Ursachen und Füllung glazial übertiefter Talabschnitte an Beispielen in den Ostalpen. Eiszeit. Gegenw. 29, 9–22.
Van Husen, D., 1983. General sediment development in relation to the climatic changes during Würm in the eastern Alps. In: Evenson, E.B., Schlüchter, Ch., Rabassa, J. (Eds.), Tills and Related Deposits. A.A. Balkema, Rotterdam, The Netherlands, pp. 345–349.
Van Husen, D., 1987. Die Ostalpen in den Eiszeiten. Geological Survey of Austria, Vienna (24 pp., 1 map.).
Van Husen, D., 2000. Geological processes during the Quaternary. Mitt. Österr. Geol. Ges. 92, 135–156.
Van Husen, D., 2004. Quaternary glaciations in Austria. In: Ehlers, J., Gibbard, P.L. (Eds.), Quaternary glaciations — extent and chronology. Developments in Quaternary Science, 2. Elsevier, Amsterdam, pp. 1–13.
Van Husen, D., Reitner, J., 2011. An outline of the Quaternary stratigraphy of Austria. E&G Quat. Sci. J. 60, 366–387.
von Wolf, H., 1922. Beiträge zur Kenntnis der eiszeitlichen Vergletscherung des Achenseegebietes in Tirol. Mitteilungen der Geographischen Gesellschaft in München, 15, pp. 147–304.
Wagner, R., 1958. Technischer Bericht zum Projekt Steinbergerache. Forstliche Abteilung für Wildbach- und Lawinenverbauung, Innsbruck (8 pp.).
Wang, X., Neubauer, F., 1998. Orogen-parallel strike-slip faults bordering metamorphic core complexes: the Salzach–Enns fault zone in the eastern Alps, Austria. J. Struct. Geol. 20, 799–818.
Whipple, K.X., 2004. Bedrock rivers and the geomorphology of active orogens. Ann. Rev. Earth Planet. Sci. 32, 151–185.
Whipple, K.X., Tucker, G.E., 1999. Dynamics of the stream-power river incision model: implications for height limits of mountain ranges, landscape response timescales, and research needs. J. Geophys. Res. 104B, 17661–17674.
Whipple, K.X., Tucker, G.E., 2002. Implications of sediment-flux-dependent river incision models for landscape evolution. J. Geophys. Res. 107 (B2), 2039. http://dx.doi.org/10.1029/2000JB000044.
Whipple, K.X., Snyder, N.P., Dollenmayer, K., 2000. Rates and processes of bedrock incision by the upper Ukak River since the 1912 Novarupta ash flow in the Valley of Ten Thousand Smokes, Alaska. Geology 28, 835–838.
Wischounig, L., 2006. Das Quartär bei Steinberg am Rofan (Tirol): Stratigraphie, Sedimentologie und Aspekte der Landschaftsentwicklung. (Diploma thesis) University of Innsbruck, Austria (105 pp., 118 figs., 12 enclosures, 1 map.).
Wohl, E.E., Merritt, D.M., 2001. Bedrock channel morphology. Geol. Soc. Am. Bull. 113, 1205–1212.
Wohl, E.E., Thompson, D.M., Miller, A.J., 1999. Canyons with undulating walls. Geol. Soc. Am. Bull. 111, 949–959.